Ore Geology Reviews xxx (2008) xxx–xxx

Contents lists available at ScienceDirect

Ore Geology Reviews

journal homepage: www.elsevier.com/locate/oregeorev

Geochronological framework and Pb, Sr isotope geochemistry of the Qingchengzi Pb–Zn–Ag–Au orefield, Northeastern China

Gang Yu [a,1], Jiangfeng Chen [a,*], Chunji Xue [b], Yuchuan Chen [c], Fukun Chen [d], Xiaoyue Du [a]

[a] Chinese Academy of Sciences Key Laboratory of Crust-Mantle Materials and Environments, School of Earth and Space Sciences, University of Science and Technology of China, Hefei 230026, PR China
[b] State Key Laboratory of Geological Processes and Mineral Resources, School of Earth Sciences and Resources, China University of Geosciences, Beijing 100083, PR China
[c] Chinese Academy of Geological Sciences, Beijing 100037, PR China
[d] Beijing Institute of Geology and Geophysics, Chinese Academy of Sciences, Beijing 100029, PR China

ARTICLE INFO

Article history:
Received 20 July 2007
Received in revised form 4 October 2008
Accepted 13 November 2008
Available online xxxx

Keywords:
Rb–Sr step-dissolution
Rb–Sr dating
Zircon U–Pb dating
Pb and Sr isotopes
Source(s) of the ore-forming materials
Qingchengzi Pb–Zn–Ag–Au orefield
Northeastern China

ABSTRACT

The Qingchengzi orefield in northeastern China, is a concentration of several Pb–Zn, Ag, and Au ore deposits. A combination of geochronological and Pb, Sr isotopic investigations was conducted. Zircon SHRIMP U–Pb ages of 225.3 ± 1.8 Ma and 184.5 ± 1.6 Ma were obtained for the Xinling and Yaojiagou granites, respectively. By step-dissolution Rb–Sr dating, ages of 221 ± 12 Ma and 138.7 ± 4.1 Ma were obtained for the sphalerite of the Zhenzigou Zn–Pb deposit and pyrargyrite of the Ag ore in the Gaojiabaozi Ag deposit, respectively. Pb isotopic ratios of the Ag ore at Gaojiabaozi ($^{206}Pb/^{204}Pb$ = 18.38 to 18.53) are higher than those of the Pb–Zn ores ($^{206}Pb/^{204}Pb$ = 17.66 to 17.96; Chen et al. [Chen, J.F., Yu, G., Xue, C.J., Qian, H., He, J.F., Xing, Z., Zhang, X., 2005. Pb isotope geochemistry of lead, zinc, gold and silver deposit clustered region, Liaodong rift zone, northeastern China. Science in China Series D 48, 467–476.]). Triassic granites show low Pb isotopic ratios ($^{206}Pb/^{204}Pb$ = 17.12 to 17.41, $^{207}Pb/^{204}Pb$ = 15.47 to 15.54, $^{208}Pb/^{204}Pb$ = 37.51 to 37.89) and metamorphic rocks of the Liaohe Group have high ratios ($^{206}Pb/^{204}Pb$ = 18.20 to 24.28 and 18.32 to 20.06, $^{207}Pb/^{204}Pb$ = 15.69 to 16.44 and 15.66 to 15.98, $^{208}Pb/^{204}Pb$ = 37.29 to 38.61 and 38.69 to 40.00 for the marble of the Dashiqiao Formation and schist of the Gaixian Formation, respectively).

Magmatic activities at Qingchengzi and in adjacent regions took place in three stages, and each contained several magmatic pulses: ca. 220 to 225 Ma and 211 to 216 Ma in the Triassic; 179 to 185 Ma, 163 to 168 Ma, 155 Ma and 149 Ma in the Jurassic, as well as ca. 140 to 130 Ma in the Early Cretaceous. The Triassic magmatism was part of the Triassic magmatic belt along the northern margin of the North China Craton produced in a post-collisional extensional setting, and granites in it formed by crustal melting induced by mantle magma. The Jurassic and Early Cretaceous magmatism was related to the lithospheric delamination in eastern China. The Triassic is the most important metallogenic stage at Qingchengzi. The Pb–Zn deposits, the Pb–Zn–Ag ore at Gaojiabaozi, and the gold deposits were all formed in this stage. They are temporally and spatially associated with the Triassic magmatic activity. Mineralization is very weak in the Jurassic. Ag ore at Gaojiabaozi was formed in the Early Cretaceous, which is suggested by the young Rb–Sr isochron age, field relations, and significantly different Pb isotopic ratios between the Pb–Zn–Ag and Ag ores. Pb isotopic compositions of the Pb–Zn ores suggest binary mixing for the source of the deposits. The magmatic end-member is the Triassic granites and the other metamorphic rocks of the Liaohe Group. Slightly different proportions of the two end-members, or an involvement of materials from hidden Cretaceous granites with slightly different Pb isotopic ratios, is postulated to interpret the difference of Pb isotopic compositions between the Pb–Zn–(Ag) and Ag ores. Sr isotopic ratios support this conclusion. At the western part of the Qingchengzi orefield, hydrothermal fluid driven by the heat provided by the now exposed Triassic granites deposited ore-forming materials in the low and middle horizons of the marbles of the Dashiqiao Formation near the intrusions to form mesothermal Zn–Pb deposits. In the eastern part, hydrothermal fluids associated with deep, hidden Triassic intrusions moved upward along a regional fault over a long distance and then deposited the ore-forming materials to form epithermal Au and Pb–Zn–Ag ores. Young magmatic activities are all represented by dykes across the entire orefield, suggesting that the corresponding main intrusion bodies are situated in the deep part of the crust. Among these, only intrusions with age of ca. 140 Ma might have released sufficient amounts of fluid to be responsible for the formation of the Ag ore at Gaojiabaozi.

* Corresponding author.
E-mail address: cjf@ustc.edu.cn (J.F. Chen).
[1] Present address: Department of Earth and Planetary Sciences, Harvard University, Cambridge, MA 02138, USA.

0169-1368/$ – see front matter
doi:10.1016/j.oregeorev.2008.11.009

Our age results support previous conclusions that sphalerite can provide a reliable Rb–Sr age as long as the fluid inclusion phase is effectively separated from the "sulfide" phase. Our work suggests that the separation can be achieved by a step-resolution technique. Moreover, we suggest that pyrargyrite is a promising mineral for Rb–Sr isochron dating.

1. Introduction

The Qingchengzi orefield, situated in eastern Liaoning Province, northeastern China (123°37' E, 40°44' N), is an important region with clusters of Pb, Zn, and precious metal deposits. The orefield contains more than ten Pb–Zn deposits and has a mining history of more than 400 years. One silver deposit and four gold deposits were recently found in the eastern part of the orefield. All these deposits are hosted by Paleoproterozoic metamorphic rocks. Orefield reserves are estimated at ca. 1.5 Mt of Pb and Zn metals, 2000 ton of Ag metal, and 100 ton of Au metal. The orefield in which the Pb, Zn, Ag, and Au deposits are concentrated is also the location of magmatism of different ages, ranging from Proterozoic, Yindosinian (Triassic) and Yanshanian (Jurassic and Cretaceous). These features have attracted attention from economic geologists.

While much work on the origin of these deposits has been carried out, discrepancies as to the ages and the metal sources of the deposits remain. Early work regarded the Qingchengzi Pb and Zn deposits as medium- to low-temperature magmatic hydrothermal deposits (103GT, 1976). Several models have been postulated since then, including a metamorphic origin model (Zhang, 1984), a Proterozoic sea floor exhalation model (Wang et al., 1994), a sedimentation–metamorphism–hydrothermal reworking model (Jiang, 1987, 1988; Jiang and Wei, 1989; Ding et al., 1992), a Mesozoic hydrothermal mineralization model (Liu and Ai, 2002; Xue et al., 2003) and many others.

Three metallogenic pulses, i.e., 190 to 160 Ma, ca. 140 Ma, and ca. 120 Ma, have been identified in northern China. Mineralization in the northern margin of the North China Craton developed in all three stages, while gold deposits in other parts of northern China mostly formed at ca. 140 Ma and ca. 120 Ma (Yang et al., 2003; Mao et al., 2005). It is unclear whether the mineralization at Qingchengzi fits into this scenario. How the mineralization at Qingchengzi relates to the geodynamic evolution of the North China Craton is also not yet known. Precise dating of the ore deposits and the country rocks, as well as study of the source(s) of the ore-forming materials, are crucial for a deeper understanding of the ore-forming process and for further prospecting.

Little geochronological work on the ores has been carried out at Qingchengzi. The ore deposits at Qingchengzi lack minerals commonly used by traditional radioactive dating methods, and the Os concentrations of the ore-forming minerals in the deposits are extremely low. Recently, Triassic and Jurassic ages for Au and Ag deposits were reported at Qingchengzi by Rb–Sr and Ar–Ar dating of fluid inclusions in the quartz and sericite (Liu and Ai, 2002; Xue et al., 2003). Further geochronological work is needed to demonstrate the mineralization ages for the Au and Ag deposits and to constrain the time of formation of the Pb and Zn deposits. Many studies have shown that Rb–Sr dating of sulfide minerals, especially sphalerite and pyrite, can be used to determine the formation age of hydrothermal sulfide mineral deposits (Nakai et al., 1990; Brannon et al., 1992; Nakai et al., 1993; Christensen et al., 1995a,b; Yang and Zhou, 2001; Wei et al., 2003; Hou et al., 2006; Han et al., 2007).

As a major component of the Pb and Zn deposits, Pb isotopes can be used to directly trace the source of the ore-forming material and to delineate the evolutionary history and the origin of Pb and Zn deposits. On the other hand, as a chalcophile element, Pb isotopes can be used to indirectly infer the source of the ore-forming material and the origin of other sulfide deposits (Zhang, 1995; Bouse et al., 1999; Chu et al., 2001; Marcoux et al., 2002). Extensive Pb isotopic studies have been carried out on the deposits at the Qingchengzi orefield (Chen et al., 1980; Jiang, 1987; Ding et al., 1992; Fang et al., 1994). However, the data produced in the 1960's and 1970's were not precise enough (Ding et al., 1992), necessitating a new Pb isotopic study (Chen et al., 2005).

In this paper, we report the results of zircon U–Pb dating of the granitic intrusions and on step-dissolution Rb–Sr dating of sulfide minerals carried out with the aim of constructing a geochronological framework for the orefield. We also present the results of Pb and Sr isotopic studies of the ores and country rocks in order to constrain the possible source(s) of the ore-forming materials and determine the origin of various ore deposits at the Qingchengzi orefield.

2. Geologic setting

The Qingchengzi orefield is situated in the Paleoproterozoic Liaodong rift zone in the eastern part of Liaoning Province (Fig. 1). This intracontinental rift developed on the Archaean North China Craton and formed through the processes of crust extension, rapid subsidence, and compression folding in the Paleoproterozoic (Fang et al., 1994). The rift zone trends NEE with a total length of ca. 700 km, is truncated by the Tanlu fault in the west, and runs into the Sea of Japan to the east. The rift zone can be divided into three tectono-lithofacies belts: the northern marginal slop, the central depression and the southern marginal slop. The orefield is located in the central depression (Fig. 1). The metamorphic rocks of the Archaean Anshan Group comprise the basement of the rift zone. The thick Paleoproterozoic Liaohe Group was deposited on the basement and is disconformably overlain by the Paleoproterozoic quartzite of the Yushulazi Group. The lower Liaohe Group, consisting of the Yujiabaozi and Langzishan Formations, comprises volcanoclastic rocks, while the upper Liaohe Group, including the Dashiqiao and Gaixian Formations, includes carbonate and clastic rocks with some volcanic interdeds. The rocks in the Liaohe Group experienced metamorphism from greenschist to amphibolite facies at ca. 1800 Ma, forming amphibolite, granulite, schist, and marble (Jiang, 1987; Fang et al., 1994; Chen et al., 2005). Recently, Faure et al. (2004) and Lu et al. (2006) postulated a hypothesis that the region studied was a Paleoproterozoic orogenic belt, probably developed at approximately 1.93 to 1.90 Ga.

Mesoproterozoic magmatism in this rift region is represented by gabbro–diabase dykes and granitic stocks (Liu, 1998). Many Triassic igneous rocks, including syenite and granite, occur in the eastern part of the Triassic magmatic belt along the northern margin of the North China Craton (Liu, 1998; Yan et al., 1999; Wu et al., 2005c). Jurassic and Early Cretaceous igneous activities are widespread in the whole rift region, as in the entire eastern China (Liu, 1998; Wu et al., 2005a,b).

The Qingchengzi orefield is covered by the Dashiqiao and Gaixian Formations of the Upper Liaohe Group. The Dashiqiao Formation can be divided into several horizons. They are, from the base to the top: D1, consisting of graphite-bearing marble; D2 garnet mica schist; D31 interbeded granulite and banded marble with tremolite marble; D32 mica schist and mica sillimanite schist; D33 dolomite marble and tremolite marble; D34 leucoleptite and schist; and D35 dolomite marble and calcite marble. They were metamorphosed from limestone and interbeded sandstone and minor volcanic rocks. The Gaixian Formation is comprised of schist with thin interbeds of marble at the base, which were metamorphosed from sandstone, volcanic rocks, and limestone interbeds (Fang et al., 1994).

Please cite this article as: Yu, G., et al., Geochronological framework and Pb, Sr isotope geochemistry of the Qingchengzi Pb–Zn–Ag–Au orefield, Northeastern China, Ore Geology Reviews (2008), doi:10.1016/j.oregeorev.2008.11.009

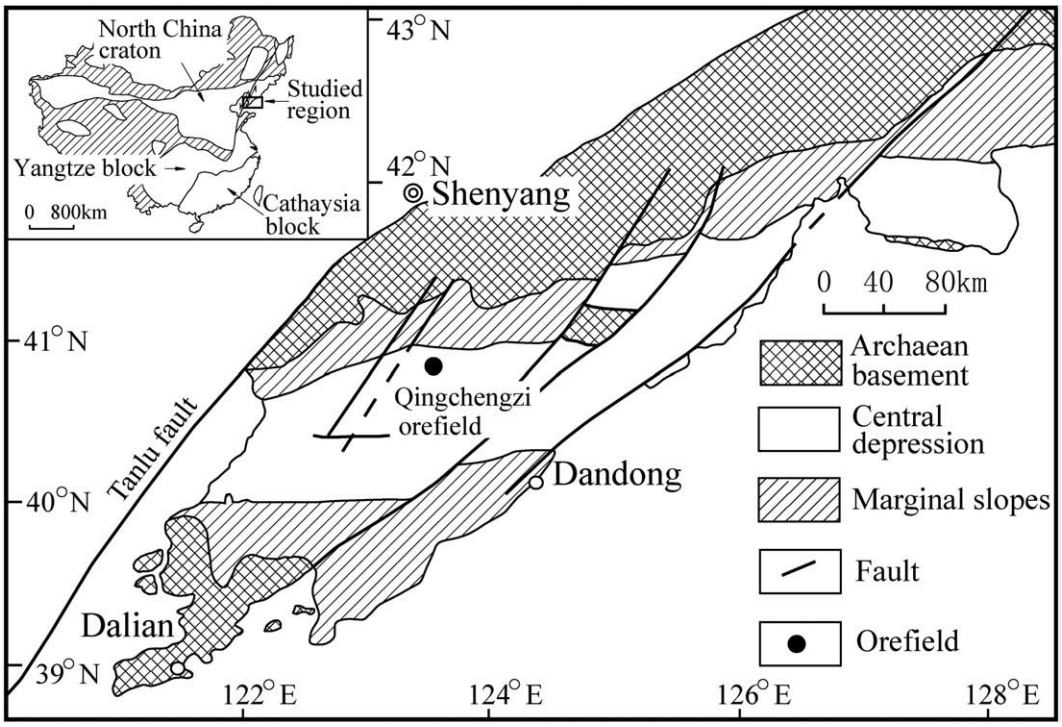

Fig. 1. Sketch map of the Proterozoic Liaodong rift zone with the location of the Qingchengzi orefield (modified after Wang and Qu, 2000).

The Paleoproterozoic metamorphic rocks form gentle folds trending east–west within the Qingchengzi orefield. Two sets of faults, striking NE and NW, respectively, cut through the metamorphic beds and spatially control the distribution of the ore deposits in the orefield. For example, all silver and gold deposits occur along the NNW-trending Jianshanzi fault. Some faults are filled by dykes with different lithologies and ages (Geological Institute of Non-ferrous Metal Deposits of Liaoning Province, 1990; Fig. 2).

Extensive multi-stage magmatism developed in the Qingchengzi region. The orefield is surrounded by granitoids of different ages which intruded into the Paleoproterozoic metamorphic rocks. The aeromagnetic interpretation and gravimetric data suggest that granites underlay the entire orefield (Fang et al., 1994).

The Proterozoic granite is represented by the Dadingzi biotite granite, located in the southeast portion of the orefield and in the middle of the field (Fig. 2). They intruded into the Paleoproterozoic Dashiqiao and Gaixian Formations. The Dadingzi rock body shows a gneissic texture and yields K–Ar ages of 1740 to 1621 Ma (103 GT, 1976). The rock is composed of plagioclase (oligoclase, 60 to 65%), potassium feldspar (15 to 20%), quartz (20 to 25%), and biotite (ca. 5%), and shows an enrichment of Na_2O over K_2O, with Na_2O/K_2O ratios of 1.5 to 2.9 (Liu, 1998). The rocks are very low in rare earth elements, with total REE of only 3.7 to 32 ppm, but show a light REE enriched pattern (LREE/HREE = 2.14; Wei, 2001).

Triassic magmatism was active at Qingchengzi and is represented by the Xinling and Shuangyashan granites as well as the Laojiandingshan diorite south of Shuangdinggou (Wu et al., 2005c). The Xinling stock and Shuangdinggou batholith crop out at the north and the southwest of the orefield, respectively (Fig. 2). They both show porphyritic textures. The Xinling body yields K–Ar ages of 218 to 227 Ma, and the Shuangdinggou 231 ± 5 Ma (Fang et al., 1994). The Xinling granite is composed of potassium feldspar (5 to 10% as phenocryst, 50 to 55% as groundmass), plagioclase (15 to 20%), quartz (20 to 25%), biotite (ca. 5%), and minor hornblende, and shows an enrichment of potassium over sodium with a Na_2O/K_2O ratio of 0.5 to 0.9. The Shuangdinggou granite is composed of potassium feldspar (10 to 15% as phenocryst, 10 to15% as groundmass), plagioclase (40 to 45%), quartz (20 to 25%), biotite (5 to 10%), and hornblende (ca. 5%), and has a Na_2O/K_2O ratio of 1.0 to 1.3. The two rock bodies show similar total REE concentrations of 140 to 190 ppm and strongly LREE enriched patterns (LREE/HREE of 10 to 12; Wei, 2001).

The Yaojiagou granite occurs as a very small plug (Fig. 2); it is a typical granite. It contains total REE of 72 ppm and a mildly LREE enriched pattern with a LREE/HREE ratio of 2.75 (Wei, 2001), which is different from that of the Triassic granites.

More than 1000 dykes occur in the orefield. They are Triassic to Early Cretaceous in age (Fang et al., 1994; Liu and Ai, 2002) and lamprophyre, gabbro–diabase, diorite, granite–porphyry and quartz–porphyry in composition (Liu, 1998). They mostly intruded along the NE and NW striking faults (Fig. 2). The post-ore-forming unaltered lamprophyres are composed of augite, biotite, potassium feldspar, and occasional amphibole. They are alkaline rocks with SiO_2 content of 43.0 to 49.5%, Na_2O+K_2O of 6.2 to 8.6% and K/(Na+K) ratio of 0.42 to 0.60. The unaltered lamprophyres show high concentrations of REE and incompatible elements with total REE of 440 to 670 ppm and very strongly LREE enriched patterns (LREE/HREE = 20–40; Liu et al., 1997). Most lamprophyres are heavily altered. A microdiorite is fine-grained with the grain size of ca. 0.5 mm. The rock is composed by plagioclase and small amount of biotite and pyrite.

Pb–Zn deposits, such as those at Xiquegou and Benshan, occur in the west of the orefield. These deposits contain more Pb than Zn and show Pb/Zn ratios of about 4. Zn–Pb deposits, such as those at Zhenzigou in the east of the field, are relatively Zn enriched with Pb/Zn ratios ranging from 1 to 0.5. Further eastward, Au and Ag deposits, including the Gaojiabaozi Ag–Pb–Zn deposit, the Xiaotongjiabaozi and Baiyun gold deposits, and several others, occur along the Jianshanzi fault (Fig. 2; Liu and Ai, 2002; Xue et al., 2003).

Three types of Pb–Zn–(Ag) orebodies have been recognized in the Qingchengzi orefield: (i) Conformable layer and lens bodies occur in the lower part (D1 horizon) and sometimes in the D33 horizon of the Dashiqiao Formation, especially around the interbeds of the granulite and schist in the east part of the field. Orebodies of this type are 50 to 200 m long and 0.5 to 5 m thick. They contain relatively low grade ore (average 2.7% Pb, 2.6% Zn). (ii) Veins and irregular bodies cutting

Please cite this article as: Yu, G., et al., Geochronological framework and Pb, Sr isotope geochemistry of the Qingchengzi Pb–Zn–Ag–Au orefield, Northeastern China, Ore Geology Reviews (2008), doi:10.1016/j.oregeorev.2008.11.009

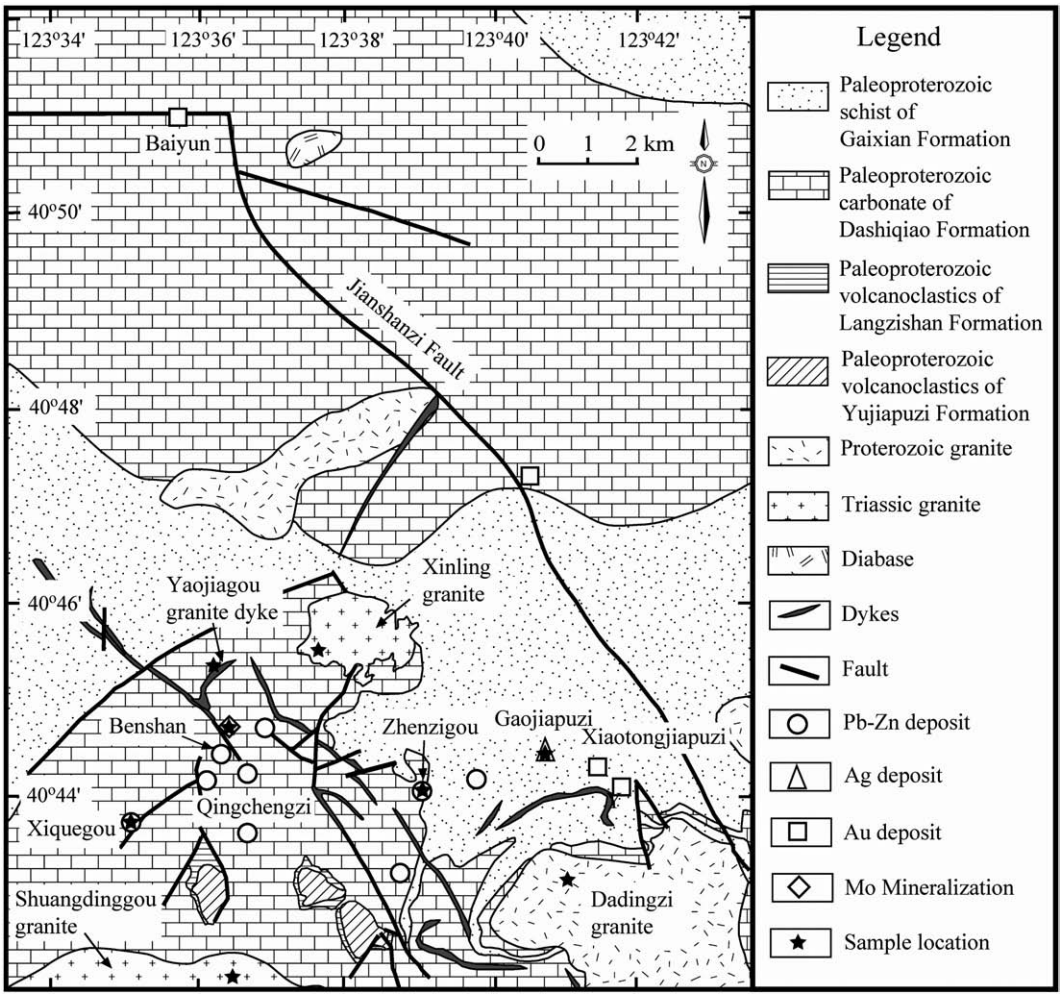

Fig. 2. Sketch geological map of the Qingchengzi orefield (after Geological Institute of Non-ferrous Metal Deposits of Liaoning Province, 1990).

through the marble occur in the western part of the field. A single body is 30 to 400 m long and 1 to 30 m thick. They usually contain high Pb (4.4%) and low Zn (1.0%). (iii) The composite bodies partially developed along a fault and partially in interbed fractures also occur in the western part of the orefield (Fang et al., 1994; Xue et al., 2003). The ores can be rich, especially in Pb, with Pb content as high as 5.9%. The type ii and iii orebodies are hosted by interbeded dolomite marble, banded mica schist, and marble, granulite, calcite marble, and sillimanite mica schist of horizon D33. For the all three types of the orebodies, country rock alteration is weak and can only be observed near the orebodies (generally within 1 to 3 m). The type of the country rock alteration, such as silicification, sericitization, dolomatization, and carbonation, is closely related to the composition of the country rocks (Fang et al., 1994). The type ii and iii ores contain Ag of ca. 50 to 100 g/t.

The Ag and Au deposits fill in interbed fractures in the schist, granulite, and marble of the uppermost horizons (D34 and D35) of the Dashiqiao Formation and near the lowest horizon of the Gaixian Formation. These Ag–Au ores are associated with silicification, potash-alteration, and late carbonation.

The Xiquegou Pb–Zn, Zhenzigou Zn–Pb, and Gaojiabaozi Ag–Pb–Zn deposits are chosen for this study.

Orebodies of the Xiquegou Pb–Zn deposit are controlled by steeply dipping faults striking NNE, NW and NE, which cut through the Dashiqiao beds. Most ores fill the faults and sometimes the interbed fractures in the marble with interlayered granulite and schist of the D3 horizon of the Dashiqiao Formation. The ore minerals include galena and sphalerite, minor pyrite, chalcopyrite, arsenopyrite, and tetrahedrite, as well as trace silver and gold minerals. The ores contain about 6% Pb and 1.5% Zn, with Pb/Zn ratio of about 4, as well as, about 100 g/t Ag (Liu et al., 2001). Four mineralization stages were recognized: they are, from early to late, high temperature dolomite, sulfide, quartz–carbonate–sulfide, and late carbonate stages. Pyrite crystallized in all four stages, but decreases in amount from the early to late stages. Sphalerite crystallized in the sulfide and quartz–carbonate–sulfide stages. Galena crystallized slightly later than the sphalerite and finished in the carbonate stage. Euhedral and subhedral sulfide minerals fill the fractures and sometimes grow around the breccia of the wall rocks. Aggregates of sulfides replace the wall rock and form the banded features. Pyrite and sphalerite are sometimes replaced by galena. Galena and chalcopyrite sometimes fill in the cracks of the pyrite. Galena decreases and sphalerite increases in orebodies from the upper to the lower horizons. The wall rock alteration includes silicification, carbonation and sericitization (Fang et al., 1994).

Zhenzigou is a typical conformable stratiform deposit which consists of layered and lens Zn–Pb orebodies. The orebodies occurring in interbed fractures are strictly controlled by the folded bedding and are hosted by graphite-bearing marble and interbeded banded graphite-bearing marble, amphibolite, and biotite schist of the D1 horizon of the Dashiqiao Formation. Ore minerals are pyrite, pyrrhotite, sphalerite and galena, with minor arsenopyrite, marcasite, and argentite. The gangue minerals include dolomite and calcite, which are very similar to that of the wall rock. The ores contain ca. 2%

Please cite this article as: Yu, G., et al., Geochronological framework and Pb, Sr isotope geochemistry of the Qingchengzi Pb–Zn–Ag–Au orefield, Northeastern China, Ore Geology Reviews (2008), doi:10.1016/j.oregeorev.2008.11.009

to 6% Pb and 2% to 10% Zn, with a Pb/Zn ratio of about 1 to 0.5, as well as ca. 50 g/t Ag. Sulfide and the gangue minerals form rhythmic lamina. Sulfide minerals are disseminated in the schist and granulite. Most sulfide minerals are euhedral and subhedral, but framboidal pyrite and micro-framboidal sphalerite can be occasionally seen. Pyrite and sphalerite are sometimes distributed around the detrital dolomite particles. Wall rock alteration is weak (Fang et al., 1994; Liu et al., 2001).

At Gaojiabaozi Ag–Pb–Zn deposit, the lenticular and tabular orebodies occur along the interlayer fractures in the interbeded marble, schist, and granulite within the uppermost horizons (D34 and D35) of the Dashiqiao Formation. Small rich orebodies sometimes occur as veins and pockets. Two types of ores (Pb–Zn–Ag and Ag) are identified. The Pb–Zn–Ag ore is massive, similar to that of the Xiquegou and Zhenzigou deposits, and contains mainly pyrite, sphalerite (dark-colored), galena, and minor chalcopyrite, arsenopyrite, native silver, tetrahedrite, pyrargyrite, and andorite. This type of ore has gradational borders, depending on cut-off grades. The Ag ore occurs in fractured marble cemented by quartz and dolomite veinlets. Breccia structures and miarolitic cavities are common, and native silver has developed in the cavities. It contains small amount of sulfides, including pyrargyrite, native silver, tetrahedrite, β-argentite, stephanite, pyrite, sphalerite (light-colored), galena, and andorite. The Ag ores occur in the fracture zones and are obviously later than the Pb–Zn–Ag ore. The ores contain Ag of 100 to 300 g/t. The most important wall rock alteration is silicification, which forms the siliceous rock and the quartz stockwork (Liu et al., 2001; Wei, 2001).

3. Analytical methods

3.1. Zircon U–Pb dating

Zircons separated from granitic bodies were analyzed using the SHRIMP II in the Beijing SHRIMP Center by procedures described by Compston et al. (1992). The age was calibrated against a reference zircon (TEM) with an age of 417 Ma. U and Th concentrations were measured using the reference zircon SL13 (age of 572 Ma, U of 238 ppm). Data were calculated using Squid 1.0 and ISOPLOT (Ludwig, 1997). Common Pb was corrected based on the measured ^{204}Pb. The average weighted ^{206}Pb/^{238}U age was yielded at a confidence level of 95%. Before analyzing, cathodoluminescence (CL) imaging was carried out in the Microprobe Laboratory, Chinese Academy of Geological Sciences, in order to investigate the internal features of the zircon.

3.2. Rb, Sr, Sm, Nd concentrations and Sr, Nd isotopic compositions

Analyses of Rb, Sr, Sm, Nd concentrations and Sr, Nd isotopic compositions were carried out at the Chinese Academy of Sciences (CAS) Key Laboratory of Crust–Mantle Materials and Environments (LCMME), University of Science and Technology of China (USTC). Subsamples were split from one single hand specimen (Yang and Zhou, 2001) and mineral concentrations were separated from the subsamples (better than 98% purity). Silicate and carbonate samples were cleaned and then powdered by a non-contaminated device and dissolved in mixed acid ($HF+HNO_3$) for silicate mineral samples and ($HCl+HNO_3$) for carbonate mineral samples in sealed Savillex beakers on a hot plate.

Two representative sulfide minerals (pyrite 300Fe from Gaojiabaozi and sphalerite ZZG-7 from Zhenzigou) were selected for testing the step-dissolution procedures (Milli Q water, 0.1, 0.2, 0.4, 0.8, 1.5, 3.0, 6.0 M HCl, aqua regia, and $HF+HNO_3$). The results are shown in Fig. 3. High Rb and Sr concentrations occur in pyrite in two fractions, in H_2O+ 0.1 M HCl and in aqua regia. They are interpreted as the fluid inclusion (termed inclusion hereafter) and sulfide phases, respectively. High Rb and Sr concentrations occur in sphalerite in three fractions, in H_2O+ 0.1 M HCl, in aqua regia, and in $HF+HNO_3$. They are interpreted as the inclusion, sulfide and silicate inclusion (termed silicate hereafter) phases, respectively. However, the actual state of Rb and Sr in the sulfide phase is not clear, and merits further investigation (Pettke and Diamond, 1996). Based on these results, sulfide minerals were first dissolved by 0.2 M HCl for 0.5 h to obtain an inclusion phase and followed by aqua regia for 24 h for the sulfide phase, and by $HF+HNO_3$ for another 24 h for the silicate phase of the sphalerite samples. Isotope spikes were then added to each solution.

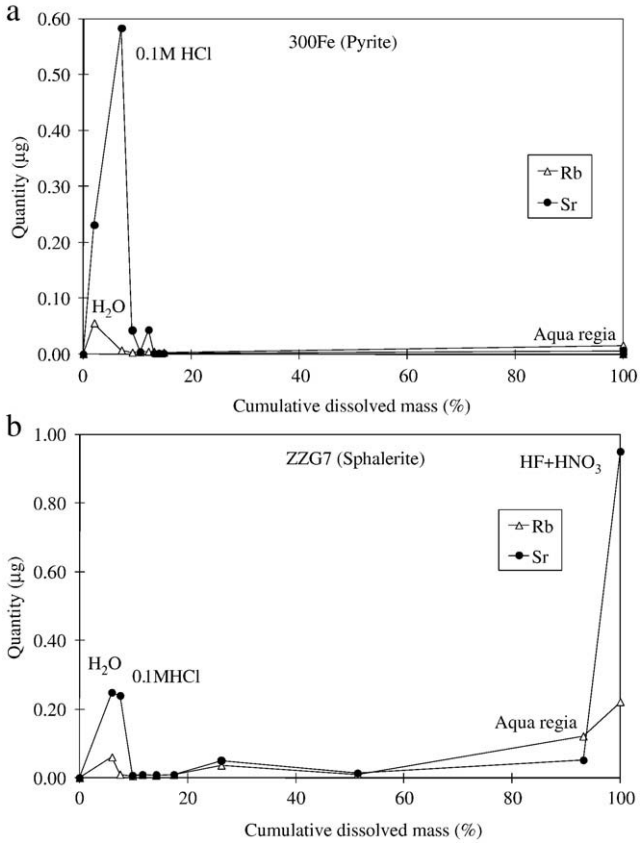

Fig. 3. The results of the step-dissolution experiments of the pyrite sample 300Fe (a) and sphalerite ZZG-7 (b).

Separation of Rb, Sr, and REE was performed via a routine ion exchange technique using Bio-Rad 50×8 cation resin. Sm and Nd were further separated from the REE fractions by an HDEHP column. Rb, Sr, Sm, and Nd concentrations were analyzed by isotope dilution (Foland and Allen, 1991). Concentrations of Rb and Sr in different phases are all calculated by the weights of the bulk samples. Isotopic ratios were measured on a Finnigan MAT-262 mass spectrometer with 7 movable collectors. Measured isotopic ratios were normalized to ^{86}Sr/^{88}Sr= 0.119400, ^{149}Sm/^{152}Sm=0.516858, and ^{146}Nd/^{144}Nd=0.721900.

Rb–Sr isochron ages were calculated using ISOPLOT (Ludwig, 1997). Initial ^{87}Sr/^{86}Sr ratios were obtained either by the isochron calculation or were calculated by correcting for the in-situ radiogenic ^{87}Sr for individual samples when no reliable isochron was obtained. The determined ^{87}Sr/^{86}Sr ratios were taken as the initials for hydrothermal calcite because of very low ^{87}Rb/^{86}Sr ratios. Initial Nd isotopic ratios were calculated by correcting for the in-situ radiogenic ^{143}Nd for individual samples and expressed in $\varepsilon_{Nd}(T)$ notation. Two stage Nd isotopic model ages ($T_{DM\ II}$) were calculated (Liew and Hofmann, 1988). The intrusive ages of 225 Ma and 1680 Ma are taken as the second stage time for the Triassic and Proterozoic granites, respectively, and the metamorphic time of 1800 Ma for metamorphic rocks of the Liaohe Group. 0.118 is used as the crustal ^{147}Sm/^{144}Nd and 0.513151 is used as the ^{143}Nd/^{144}Nd of the depleted mantle (Chen and Jahn, 1998, 1999).

Please cite this article as: Yu, G., et al., Geochronological framework and Pb, Sr isotope geochemistry of the Qingchengzi Pb–Zn–Ag–Au orefield, Northeastern China, Ore Geology Reviews (2008), doi:10.1016/j.oregeorev.2008.11.009

Table 1
SHRIMP U-Pb results of zircons from the Xinling granite (04LN680)

No.	U	Th	Th/U	Isotopic ratios								Apparent ages (Ma)					
	(ppm)	(ppm)		$^{204}Pb/^{206}Pb$	±%	$^{207}Pb^*/^{206}Pb^*$	±%	$^{207}Pb^*/^{235}U$	±%	$^{206}Pb^*/^{238}U$	±%	$^{206}Pb/^{238}U$		$^{207}Pb/^{206}Pb$		$^{208}Pb/^{232}Th$	
1	963	479	0.50	2.9E−4	23	0.047	2.6	0.2322	2.9	0.03584	1.3	227.0	±2.9	49	±62	218.0	±5.3
2	1071	565	0.53	2.3E−4	25	0.048	2.3	0.2424	2.6	0.03656	1.3	231.4	±2.9	104	±53	225.0	±4.8
3	909	416	0.46	3.0E−4	21	0.048	2.5	0.2325	2.8	0.03538	1.3	224.1	±2.8	83	±60	212.5	±5.5
4	906	376	0.41	1.7E−4	33	0.048	2.3	0.2355	2.6	0.03530	1.3	223.6	±2.8	119	±54	214.7	±5.4
5	820	402	0.49	4.1E−4	23	0.046	3.4	0.2269	3.7	0.03557	1.3	225.3	±2.9	11	±83	213.8	±7.1
6	1312	679	0.52	2.0E−4	22	0.048	1.8	0.2422	2.2	0.03642	1.3	230.6	±2.8	111	±43	225.2	±4.3
7	869	396	0.46	7.0E−5	101	0.051	2.5	0.2491	2.8	0.03554	1.3	225.1	±2.8	233	±57	225.0	±5.6
8	955	497	0.52	2.8E−4	25	0.047	2.7	0.2327	3.0	0.03590	1.3	227.4	±2.9	50	±64	219.6	±5.3
9	1013	476	0.47	2.5E−4	29	0.048	2.6	0.2284	2.9	0.03437	1.3	217.8	±2.7	109	±61	213.0	±5.4
10	1039	525	0.51	1.9E−4	24	0.048	2.0	0.2342	2.3	0.03557	1.3	225.3	±2.8	87	±46	219.6	±4.4
11	1333	649	0.49	1.1E−4	30	0.050	1.5	0.2388	2.0	0.03469	1.3	219.9	±2.7	192	±35	217.9	±3.9
12	964	423	0.44	2.7E−4	23	0.047	2.8	0.2275	3.1	0.03491	1.3	221.2	±2.8	63	±67	205.2	±5.3

Uncertainties are given at the 1σ level. Pb* represents the radiogenic Pb. Common lead correction was carried out based on the measured ^{204}Pb.

3.3. U, Th, Pb concentrations and Pb isotopic compositions

U, Th, and Pb concentrations were analyzed at the CAS Key Laboratory of Structure Research, USTC by ICP-MS (PQ III). Pb isotopic compositions were measured at LCMME, USTC. Whole rock samples of the Proterozoic granite, metamorphic rocks, and feldspars separated from the Mesozoic granitoids were digested in Sevillex vials by HF+HNO_3, carbonate samples by HCl, and pyrargyrite by the procedure described in Section 3.2. The solution was heated until incipient dryness and was then converted to a 1.5 M HCl+0.65 M HBr solution. Pb was separated by chromatography on Bio-Rad AG-1x8 anion exchange resin. Pb isotopic ratios were analyzed on a Finnigan MAT-262 multi-collector thermal ionization mass spectrometer by static mode and silica gel was used as emission. Signals on mass 205 were measured to monitor the interference of Tl. Measured isotopic ratios were corrected for a mass fractionation of 0.096% per atomic mass unit, determined by replicate measurements of reference sample SRM 981. The determined Pb isotopic ratios for the pyrargyrite and feldspar samples were taken as the initial ratios because U and Th concentrations in those samples were very low. Initial Pb isotopic ratios for other samples were calculated by correction for in-situ radiogenic Pb isotopes.

4. Results

4.1. SHRIMP U–Pb ages of zircons from orefield granites

The SHRIMP U–Pb isotope results of the zircons separated from the Xinling and Yaojiagou granites are listed in Tables 1 and 2. Zircon grains separated from the Xinling granite (04LN680) are transparent, light yellow to light brown in color, euhedral, and have length to width ratios of 2:1 to 3:1. The grain size of the zircons is about 200 μm. CL images of the zircon grains show magmatic oscillatory zoning (Fig. 4), suggesting a magmatic origin. Th/U ratios of 12 analyses range from 0.41 to 0.53, further supporting the magmatic origin for these zircon grains (Vavra et al., 1996; Rubatto, 2002). $^{204}Pb/^{206}Pb$ ratios are low and range from 7.0×10^{-5} to 4.1×10^{-4}, suggesting that the analyses are reliable. An average $^{206}Pb/^{238}U$ age of 225.3±1.8 Ma was obtained (Fig. 4). This age agrees with the previous K–Ar ages (218 to 227 Ma; Fang et al., 1994) and is interpreted as the formation age of the granite.

Zircon grains separated from the Yaojiagou granite (04LN683) are transparent, light yellow in color, and euhedral, with length to width ratios of about 3:1. A few grains are brown in color with dirty surfaces and length to width ratios of about 1.5:1. The grain size of the zircons is about 100 to 300 μm. CL images showing magmatic oscillatory zoning (Fig. 5) and high Th/U ratios of 0.10 to 0.73 suggest a magmatic origin for these zircon grains (Vavra et al., 1996; Rubatto, 2002). $^{204}Pb/^{206}Pb$ ratios are low and range from 6.7×10^{-5} to 1.5×10^{-3}, again suggesting that the analyses are reliable. An average $^{206}Pb/^{238}U$ age of 184.5±1.6 Ma was obtained (Fig. 5) and is interpreted as the formation age of the granite. The result is not consistent with previous studies (Fang et al., 1994) which assumed that the Yaojiagou and the Xinling granites were formed at the same time, and suggests a magmatic event at about 185 Ma; however, this event is only represented by the small bodies.

4.2. Rb–Sr isotopic results of the Zhenzigou, Xiquegou, and Gaojiabaozi deposits

Rb–Sr isotopic results of the sphalerite from the Zhenzigou deposit are listed in Table 3. The inclusion phase of the sphalerite from the Zhenzigou deposit shows a low quantity of Rb (concentration of 0.01 to 0.38 ppm), but a high quantity of Sr (0.52 to 6.16 ppm) and a very low $^{87}Rb/^{86}Sr$ ratio (0.02 to 0.33, except for a single outlier of 2.09).

Table 2
SHRIMP U–Pb results of zircons from the Yaojiagou granite (04LN683)

No	U	Th	Th/U	Isotopic ratios								Apparent ages (Ma)					
	(ppm)	(ppm)		$^{204}Pb/^{206}Pb$	±%	$^{207}Pb^*/^{206}Pb^*$	±%	$^{207}Pb^*/^{235}U$	±%	$^{206}Pb^*/^{238}U$	±%	$^{206}Pb/^{238}U$		$^{207}Pb/^{206}Pb$		$^{208}Pb/^{232}Th$	
1	301	219	0.73	8.9E−4	24	0.0376	10	0.1500	10	0.02885	1.5	183.4	±2.7	−512	±270	166.2	±8.2
2	1894	219	0.12	6.7E−5	33	0.0493	1.3	0.1967	1.8	0.02892	1.2	183.8	±2.2	163	±31	183.7	±5.6
3	1510	641	0.42	9.2E−5	33	0.0494	1.5	0.1987	1.9	0.02921	1.2	185.6	±2.3	165	±34	186.2	±3.4
4	2193	394	0.18	3.4E−4	16	0.0497	1.9	0.2001	2.3	0.02923	1.2	185.7	±2.3	179	±45	176.0	±8.2
5	968	710	0.73	3.1E−4	22	0.0455	2.8	0.1806	3.1	0.02875	1.3	182.7	±2.3	−26	±68	177.4	±3.6
6	1627	217	0.13	1.8E−4	23	0.0480	1.7	0.1913	2.1	0.02888	1.2	183.5	±2.3	101	±40	156.0	±7.8
7	1662	251	0.15	2.0E−4	25	0.0476	1.9	0.1921	2.3	0.02926	1.2	185.9	±2.3	80	±46	166.9	±8.3
8	1895	191	0.10	8.9E−5	29	0.0494	1.3	0.1998	1.8	0.02935	1.2	186.5	±2.3	166	±30	171.8	±7.1
9	249	93	0.37	1.5E−3	22	0.0301	19	0.1150	19	0.02778	1.6	176.6	±2.9	−1,150	±570	107	±22
10	1236	305	0.25	2.6E−4	24	0.0493	2.3	0.1935	2.6	0.02845	1.3	180.8	±2.3	164	±53	165.4	±6.7

Uncertainties are given at 1σ level. Pb* represents the radiogenic Pb. Common lead correction was carried out based on the measured ^{204}Pb.

Please cite this article as: Yu, G., et al., Geochronological framework and Pb, Sr isotope geochemistry of the Qingchengzi Pb–Zn–Ag–Au orefield, Northeastern China, Ore Geology Reviews (2008), doi:10.1016/j.oregeorev.2008.11.009

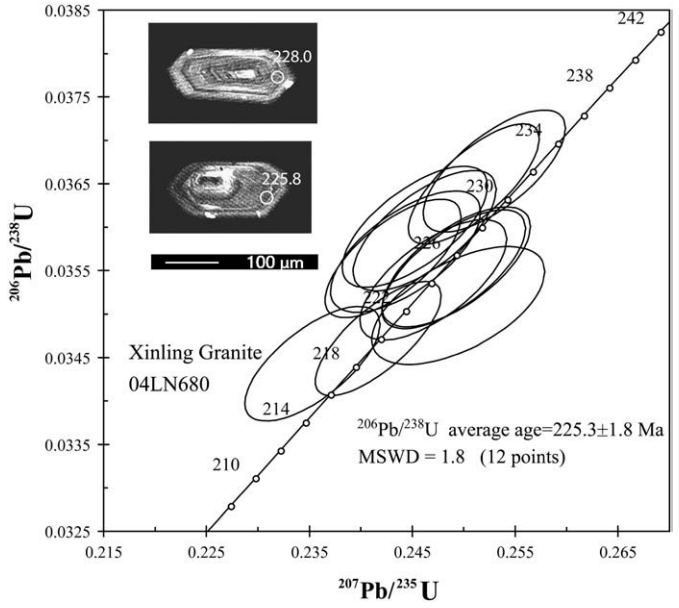

Fig. 4. Concordia diagram of the zircon from the Xinling granite.

Therefore, it does not yield any linear trend (Fig. 6). In contrast, the sulfide phase shows high Rb (0.38 to 4.38 ppm) and low Sr concentrations (0.13 to 1.18 ppm) and a variably high $^{87}Rb/^{86}Sr$ ratio (3.34 to 75.60). These data, except for two samples (ZZG-6 and -8), show a linear correlation and yield an apparent isochron age of 217 ± 26 Ma with an initial $^{87}Sr/^{86}Sr$ ratio of 0.711 ± 0.014 and a very large MSWD value. By omitting another data point (ZZG-14) which deviated from the linear trend, the improved isochron yields the age of 224 ± 14 Ma and an initial ratio 0.7053 ± 0.0078, overlapping with the ones yielded by the 6-point isochron but showing improved linearity. Combining the Rb–Sr data of the five sulfide phase samples and those of all inclusion samples, an isochron with an age of 221 ± 12 Ma and an initial isotopic ratio of 0.7075 ± 0.0063 was obtained (Fig. 6). The Rb–Sr data of the sphalerite from the Zhenzigou deposit shows a pattern very similar to that yielded by the sphalerite from the Mississippi Valley-type (MVT) deposits. The Rb–Sr isochron age obtained from the inclusion and sulfide phases of the sphalerite from the MTV deposits

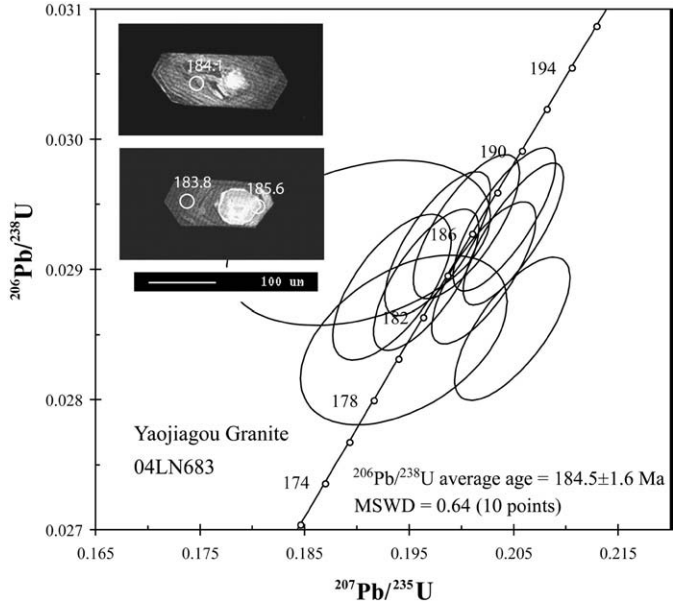

Fig. 5. Concordia diagram of the zircon from the Yaojiagou granite.

Table 3
Rb–Sr isotopic results of the sphalerite from the Zhenzigou deposit

Sample No.	Sample		Rb (ppm)	Sr (ppm)	$^{87}Rb/^{86}Sr$	$^{87}Sr/^{86}Sr$	±	$^{87}Sr/^{86}Sr$ (T)
ZZG-5	sphalerite	inclusion	0.221	4.45	0.144	0.71124	2	
ZZG-6	sphalerite	inclusion	0.346	3.051	0.328	0.71304	2	
ZZG-8	sphalerite	inclusion	0.269	6.157	0.126	0.71224	1	
ZZG-9	sphalerite	inclusion	0.010	2.025	0.015	0.71416	2	
ZZG-10	sphalerite	inclusion	0.168	3.499	0.139	0.70858	2	
ZZG-12	sphalerite	inclusion	0.375	0.519	2.089	0.71328	1	
ZZG-14	sphalerite	inclusion	0.134	5.278	0.074	0.71625	2	
ZZG-15	sphalerite	inclusion	0.121	3.325	0.106	0.71151	2	
ZZG-5	sphalerite	sulfide	2.908	0.192	44.46	0.84378	8	
ZZG-6	sphalerite	sulfide	0.966	0.193	14.57	0.78595	3	0.7075
ZZG-8	sphalerite	sulfide	1.664	0.415	11.71	0.79844	3	±0.0063
ZZG-9	sphalerite	sulfide	3.389	0.133	75.60	0.94873	10	
ZZG-10	sphalerite	sulfide	1.360	1.178	3.343	0.71485	2	
ZZG-12	sphalerite	sulfide	4.382	0.378	33.82	0.81165	2	
ZZG-14	sphalerite	sulfide	0.384	0.172	6.49	0.74363	3	
ZZG-15	sphalerite	sulfide	0.761	0.157	14.08	0.75394	5	
ZZG-5	sphalerite	silicate	0.106	1.088	0.281	0.71460	2	
ZZG-9	sphalerite	silicate	0.708	2.573	0.798	0.72520	2	

The initial isotopic ratio was obtained by isochron (Fig. 6).

was interpreted as the formation age of the deposits (Nakai et al., 1990, 1993; Brannon et al., 1992; Christensen et al., 1995a,b; Pettke and Diamond, 1996). In the same way, the age of 221 ± 12 Ma is interpreted as the formation age of the sphalerite, and, hence, of the Zhenzigou ore deposit. However, the Rb–Sr isotopic system was disturbed by one or more later thermal events because several data points deviate from the isochron. Rb–Sr data of the silicate phase is not discussed here because it is difficult to judge whether the silicate mineral inclusions and the host sulfide minerals were formed at the same time and whether they possessed the same initial isotopic ratio when they were formed.

Rb–Sr isotopic results of the pyrite and galena samples from the Xiquegou deposit are listed in Table 4. Both inclusion and sulfide phases of the pyrite and galena samples show very low Rb and Sr (concentrations <1 ppm). Rb and Sr concentrations of the inclusion and sulfide phases in the galena samples are lower than those of the pyrite samples. Rb and Sr concentrations of the inclusion phase of both the galena and pyrite are higher than in the sulfide phases in both minerals, but the $^{87}Rb/^{86}Sr$ ratio of the sulfide phase is greater than that of the inclusion phase (Table 4). Seven inclusion phase samples of the pyrite show $^{87}Rb/^{86}Sr$ ratios of 1.39–2.79 and plot along a 225 Ma reference isochron in an $^{87}Rb/^{86}Sr$–$^{87}Sr/^{86}Sr$ diagram (Fig. 7). Six sulfide-phase samples of the pyrite are more scattered and can be divided into two groups (294-3 and -4 vs. 294-1, -2, -6 and -7) with

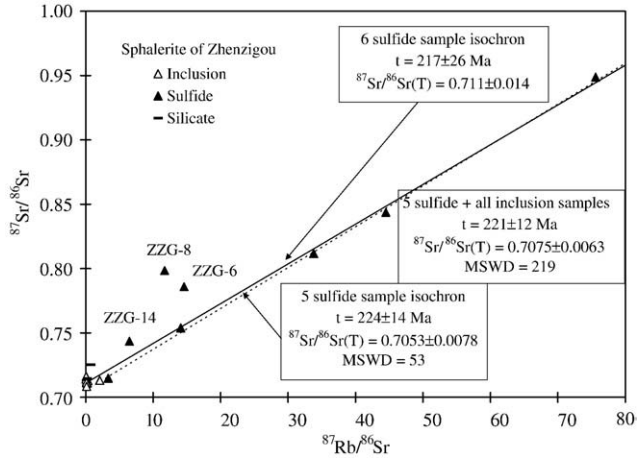

Fig. 6. $^{87}Rb/^{86}Sr$ *vs.* $^{87}Sr/^{86}Sr$ plot for the sphalerite from Zhenzigou.

Please cite this article as: Yu, G., et al., Geochronological framework and Pb, Sr isotope geochemistry of the Qingchengzi Pb–Zn–Ag–Au orefield, Northeastern China, Ore Geology Reviews (2008), doi:10.1016/j.oregeorev.2008.11.009

Table 4
Rb–Sr isotopic results of the pyrite and galena from the Xiquegou deposit

Sample No.	Sample		Rb (ppm)	Sr (ppm)	$^{87}Rb/^{86}Sr$	$^{87}Sr/^{86}Sr$	±	$^{87}Sr/^{86}Sr$ (T)
294-1	pyrite	inclusion	0.452	0.564	2.33	0.72679	2	0.71934
294-2	pyrite	inclusion	0.462	0.793	1.69	0.72274	2	0.71733
294-3	pyrite	inclusion	0.258	0.492	1.52	0.72448	2	0.71961
294-4	pyrite	inclusion	0.275	0.409	1.95	0.72444	2	0.71820
294-5	pyrite	inclusion	0.198	0.310	1.85	0.72502	2	0.71909
294-6	pyrite	inclusion	0.565	0.587	2.79	0.72663	6	0.71769
294-7	pyrite	inclusion	0.381	0.794	1.39	0.72187	2	0.71742
294-1	pyrite	sulfide	0.317	0.219	4.20	0.73442	5	0.72098
294-2	pyrite	sulfide	0.471	0.424	3.22	0.73180	3	0.72149
294-3	pyrite	sulfide	0.277	0.373	2.16	0.72182	1	0.71492
294-4	pyrite	sulfide	0.431	0.257	4.86	0.73352	4	0.71798
294-6	pyrite	sulfide	0.197	0.140	4.09	0.73486	4	0.72178
294-7	pyrite	sulfide	0.234	0.166	4.09	0.73481	2	0.72172
294-1	galena	inclusion	0.145	0.380	1.10	0.71475	1	
294-2	galena	inclusion	0.050	0.229	0.63	0.71785	4	
294-3	galena	inclusion	0.045	0.225	0.58	0.71952	2	
294-4	galena	inclusion	0.064	0.135	1.37	0.71802	2	
294-5	galena	inclusion	0.059	0.124	1.37	0.71895	2	
294-6	galena	inclusion	0.046	0.179	0.75	0.71840	2	
294-7	galena	inclusion	0.055	0.135	1.18	0.71673	6	
294-2	galena	sulfide	0.051	0.063	2.35	0.72253	2	
294-3	galena	sulfide	0.018	0.038	1.35	0.72328	3	

The initial isotopic ratios were back calculated to 225 Ma.

initials lower and higher than that yielded by the inclusion reference isochron (Fig. 7). Data from the galena samples are also scattered (Fig. 7) because they possess very low Rb and Sr concentrations, which makes galena less resisted for the late disturbance.

Rb–Sr isotopic results of minerals from Gaojiabaozi are listed in Table 5. Rb and Sr concentrations of sulfide phase samples of the pyrite in the Gaojiabaozi deposit are too low to have reliable results. The inclusion phase samples of the pyrite show low Rb (0.02 to 0.07 ppm) and moderate Sr (2.0 to 3.5 ppm), and low $^{87}Rb/^{86}Sr$ (0.01 to 0.08) and variable $^{87}Sr/^{86}Sr$ ratios (0.7215 to 0.7236). Calcite samples show a very high Sr concentration of 355 to 524 ppm, a very low $^{87}Rb/^{86}Sr$ ratio, and high and variable $^{87}Sr/^{86}Sr$ ratios (0.7259 to 0.7305). None of the pyrite and calcite samples could be used for geochronological purposes.

Sulfide phase samples of three pyrargyrite samples from the silver ore (662-1, -2 and -3; Table 5) show variable $^{87}Rb/^{86}Sr$ (0.085 to 6.6) and $^{87}Sr/^{86}Sr$ ratios (0.7196 to 0.7310). The data form an apparent isochron yielding an age of 138.7 ± 4.1 Ma with an initial $^{87}Sr/^{86}Sr$ ratio of 0.71803 ± 0.00028 (MSWD = 1.5; Fig. 8). There are two possible interpretations for the linear array given by pyrargyrite in the $^{87}Rb/^{86}Sr$ *vs.* $^{87}Sr/^{86}Sr$ plot. First of all, it could be a mixing line formed at an age older than 139 Ma, for example, at about 167 Ma ago when the K–Ar isotopic system of the sericite in the gold ore was reset, or at 221 ± 12 Ma when the Pb–Zn ores were formed. Such interpretation requires a starting line of the Rb–Sr system with a negative slop, corresponding to a mixing between a high $^{87}Sr/^{86}Sr$ component, such as that from the metamorphic rocks, and a low $^{87}Sr/^{86}Sr$ component, such as that from the granites. Secondly, it could be an isochron yielding the formation age of the mineral and, hence, the silver ore. The Ag ore was obviously formed later than the Pb–Zn–Ag ore based on the field observations, but whether the difference of the ages of the two types of ores is significantly larger than the uncertainty of the dating method is unknown. However, the Ag ore and the Pb–Zn–Ag ore show different Pb isotopic ratios (see Section 4.3), suggesting different sources and indicating that they may have formed in different geologic events. Therefore, we prefer the second interpretation. The three inclusion phase samples show somewhat scattered data, suggesting that the

Table 5
Rb-Sr isotopic results of the sulfide minerals and calcite from the Gaojiabaozi deposit

Sample No.	Sample		Rb (ppm)	Sr (ppm)	$^{87}Rb/^{86}Sr$	$^{87}Sr/^{86}Sr$	±	$^{87}Sr/^{86}Sr$(T)
Pb–Zn–Ag ore								
300Fe	pyrite	inclusion	0.066	2.456	0.078	0.72282	5	0.72257
300-1Fe	pyrite	inclusion	0.033	2.818	0.034	0.72358	2	0.72347
299-1Fe	pyrite	inclusion	0.022	2.931	0.021	0.72168	4	0.72161
299-2Fe	pyrite	inclusion	0.047	2.040	0.066	0.72175	6	0.72154
299-4Fe	pyrite	inclusion	0.019	3.151	0.017	0.72244	5	0.72239
299-5Fe	pyrite	inclusion	0.017	2.859	0.017	0.72152	5	0.72147
299-7Fe	pyrite	inclusion	0.016	3.474	0.013	0.72175	6	0.72171
300	calcite		1.165	531.6	0.006	0.73045	2	0.73043
300-1	calcite		–	369.1	0.006	0.72808	2	0.72806
299-1	calcite		–	406.6	0.006	0.72729	2	0.72727
299-2	calcite		–	483.6	0.006	0.72692	2	0.72690
299-3	calcite		–	369.1	0.006	0.72751	2	0.72749
299-4	calcite		–	387.7	0.006	0.72703	2	0.72701
299-5	calcite		–	370.1	0.006	0.72709	2	0.72707
299-6	calcite		–	355.4	0.006	0.72736	2	0.72734
299-7	calcite		–	519.6	0.006	0.72586	2	0.72584
306Ag	pyrargyrite	inclusion	0.027	0.303	0.26	0.71129	9	0.71046
Ag ore								
662-1	pyrargyrite	inclusion	0.103	1.445	0.206	0.71858	2	0.71817
662-2	pyrargyrite	inclusion	0.119	1.237	0.278	0.71996	2	0.71941
662-3	pyrargyrite	inclusion	0.084	0.575	0.42	0.71808	6	0.71725
662-1	pyrargyrite	sulfide	0.213	0.350	1.76	0.72164	2	0.71803±
662-2	pyrargyrite	sulfide	0.443	0.195	6.59	0.73101	2	0.00028
662-3	pyrargyrite	sulfide	0.154	0.527	0.845	0.71956	2	

The initial isotopic ratios of pyrite, calcite and parargyrite sample 300 were back calculated to 225 Ma and that of the other pyrargyrite inclusion samples 139 Ma. Initial Sr ratio of pyrargirite sulfide samples of the Ag ore was obtained by isochron (Fig. 8).

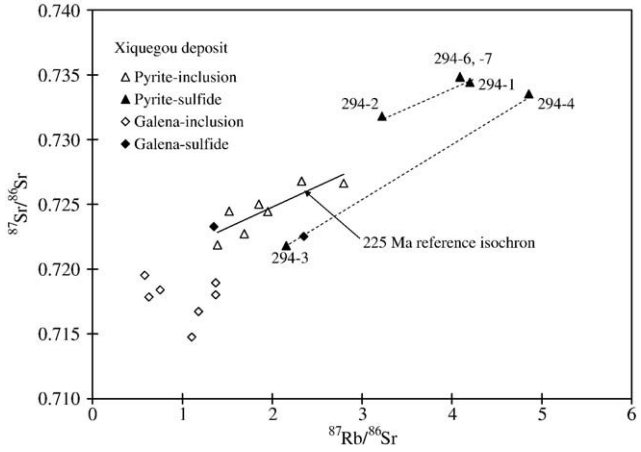

Fig. 7. $^{87}Rb/^{86}Sr$ *vs.* $^{87}Sr/^{86}Sr$ plot for pyrite and galena samples from Xiquegou.

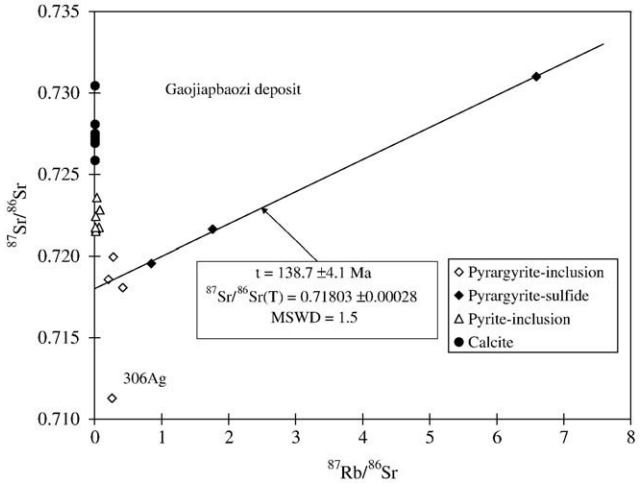

Fig. 8. $^{87}Rb/^{86}Sr$ *vs.* $^{87}Sr/^{86}Sr$ plot for pyrite, hydrothermal calcite, and pyrargyrite samples from Gaojiabaozi.

Please cite this article as: Yu, G., et al., Geochronological framework and Pb, Sr isotope geochemistry of the Qingchengzi Pb–Zn–Ag–Au orefield, Northeastern China, Ore Geology Reviews (2008), doi:10.1016/j.oregeorev.2008.11.009

Table 6
Pb isotopic results of the pyrargyrite from the Gaojiapuzi ore deposit and feldspar of the Mesozoic granite from the Qingchengzi orefield

Sample		$^{206}Pb/^{204}Pb$	+/−	$^{207}Pb/^{204}Pb$	+/−	$^{208}Pb/^{204}Pb$	+/−
Pb–Zn–Ag ore							
300		17.692	1	15.558	2	37.699	4
Ag ore							
622-1	Inclusion	18.376	1	15.651	2	37.893	4
622-1a	Inclusion	18.491	1	15.791	1	38.344	2
	Sulfide	18.405	1	15.681	2	37.987	5
622-2	Inclusion	18.421	1	15.748	1	38.221	2
	Sulfide	18.391	1	15.662	1	37.925	3
622-3	Inclusion	18.527	1	15.786	1	38.311	3
	Sulfide	18.429	1	15.665	1	37.917	3
622-4	Inclusion	18.383	1	15.653	1	37.894	3
	Sulfide	18.395	1	15.664	1	37.929	2
Shuangdinggou granite							
04LN676	Feldspar	17.410	2	15.525	2	37.874	4
04LN677	Feldspar	17.121	2	15.483	2	37.863	4
04LN678	Feldspar	17.201	2	15.471	2	37.841	6
04LN679	Feldspar	17.159	2	15.495	1	37.885	3
Xinling granite							
04LN681	Feldspar	17.208	2	15.535	2	37.510	4

Uncertainties are expressed as the last digit.

Rb–Sr isotopic system in them has been disturbed after formation. Initial $^{87}Sr/^{86}Sr$ ratios of the inclusion samples calculated by correcting for in-situ radiogenic ^{87}Sr (0.7173 to 0.7194) are close to those yielded by the isochron constructed by the sulfide phase samples, suggesting that the disturbance is limited.

4.3. Pb isotopic compositions of the ore deposits and the country rocks

Pb isotopic compositions of pyrargyrite samples from the Gaojiabaozi deposit and feldspars from Triassic granites are listed in Table 6. U, Th, and Pb concentrations and Pb isotopic ratios of the Proterozoic granites and metamorphic rocks of the Liaohe Group are shown in Table 7.

Pb isotopic ratios of pyrargyrite sample 300 from the Pb–Zn–Ag ore at Gaojiabaozi (Table 6) are within the range of those of Pb–Zn ores from the Pb–Zn deposits at Qingchengzi (Chen et al., 2005). The data plot near the evolution curve of the upper crust in the Pb isotopic plots (Fig. 9; Zartman and Doe, 1981). Pb isotopic ratios of pyrargyrite from the Ag ore of Gaojiabaozi also show small variations: $^{206}Pb/^{204}Pb = 18.38$ to 18.53; $^{207}Pb/^{204}Pb = 15.65$ to 15.79; and $^{208}Pb/^{204}Pb = 37.89$ to 38.34 (Table 6). Pb in the Ag ore shows higher $^{206}Pb/^{204}Pb$ ratios than the Pb in the Pb–Zn ores (Fig. 9; Chen et al., 2005).

Feldspar of the Xinling and Shuangdinggou granites shows $^{206}Pb/^{204}Pb = 17.12$ to 17.41, $^{207}Pb/^{204}Pb = 15.47$ to 15.54 and $^{208}Pb/^{204}Pb = 37.51$ to 37.89 (Table 6; Fig. 9). The two granites show very similar Pb isotopic ratios; this suggests that they were derived from the same source and implies that they were formed at the same time.

The Proterozoic granites show non–radiogenic Pb isotopic compositions (at 225 Ma) of $^{206}Pb/^{204}Pb$ (225 Ma) = 16.14 to 16.62, $^{207}Pb/^{204}Pb$ (225 Ma) = 15.49 to 15.53, and $^{208}Pb/^{204}Pb$ (225 Ma) = 35.77 to 36.07 (Table 7; Fig. 9). 225 Ma in-situ radiogenic Pb corrected isotopic

Table 7
U, Th, Pb concentrations and Pb isotopic ratios of the Proterozoic granite, marble of the Dashiqiao Formation and schist of the Gaixian Formation from the Qingchengzi orefield

Sample No.	Location	U (ppm)	Th (ppm)	Pb (ppm)	$^{206}Pb/^{204}Pb$	±	$^{207}Pb/^{204}Pb$	±	$^{208}Pb/^{204}Pb$	±
Proterozoic granite										
669	Dadingzi	0.17	0.73	5.87	16.678	2	15.536	2	36.155	4
670	Dadingzi	0.20	0.60	11.69	16.302	2	15.523	2	35.800	4
671	Dadingzi	0.20	0.25	9.27	16.282	2	15.514	2	35.931	5
672	Dadingzi	0.12	0.16	5.55	16.182	1	15.495	2	35.789	4
Marble of the Dashiqiao Formation										
291 g	Xiquegou	0.13	0.23	2.09	19.489	5	15.806	4	37.430	12
291y	Xiquegou	0.29	0.64	2.24	22.150	4	16.086	4	38.367	9
292 g	Xiquegou	1.16	0.77	3.85	23.724	4	16.281	2	37.928	6
292y	Xiquegou	1.55	0.98	3.08	22.635	4	16.193	4	38.107	11
296	Xiquegou	0.70	0.14	4.09	18.589	6	15.709	3	38.627	7
666a	Gaojiapuzi	0.74	0.10	1.27	25.147	6	16.485	3	37.352	8
666b	Gaojiapuzi	0.92	0.08	1.08	22.800	8	16.213	5	37.678	13
Schist of the Gaixian Formation										
663	Gaojiapuzi	4.44	13.66	11.20	20.641	3	16.003	3	39.630	7
689	Surface	2.02	10.79	16.43	18.604	2	15.672	2	39.945	5
690	Surface	1.92	10.04	8.71	19.775	3	15.823	2	40.549	5

Sample No.	Corrected for 225 Ma radiogenic Pb			Corrected for 139 Ma radiogenic Pb		
	$^{206}Pb/^{204}Pb$	$^{207}Pb/^{204}Pb$	$^{208}Pb/^{204}Pb$	$^{206}Pb/^{204}Pb$	$^{207}Pb/^{204}Pb$	$^{208}Pb/^{204}Pb$
Proterozoic granite						
669	16.616	15.533	36.069	16.640	15.534	36.102
670	16.266	15.521	35.765	16.280	15.522	35.778
671	16.236	15.512	35.912	16.254	15.513	35.920
672	16.137	15.493	35.769	16.154	15.494	35.777
Marble of the Dashiqiao Formation						
291 g	19.353	15.799	37.349	19.405	15.802	37.380
291y	21.845	16.071	38.147	21.963	16.077	38.231
292 g	22.992	16.244	37.771	23.275	16.259	37.831
292y	21.435	16.132	37.860	21.898	16.157	37.955
296	18.202	15.689	38.602	18.351	15.697	38.612
666a	23.717	16.413	37.292	24.270	16.442	37.315
666b	20.765	16.110	37.619	21.551	16.152	37.642
Schist of the Gaixian Formation						
663	19.700	15.955	38.688	20.063	15.975	39.049
689	18.320	15.658	39.451	18.430	15.663	39.641
690	19.254	15.797	39.660	19.455	15.807	40.001

Pb isotopic ratios of the samples 291 g, 291y, 292 g and 292y are from Chen et al. (2005).

Please cite this article as: Yu, G., et al., Geochronological framework and Pb, Sr isotope geochemistry of the Qingchengzi Pb–Zn–Ag–Au orefield, Northeastern China, Ore Geology Reviews (2008), doi:10.1016/j.oregeorev.2008.11.009

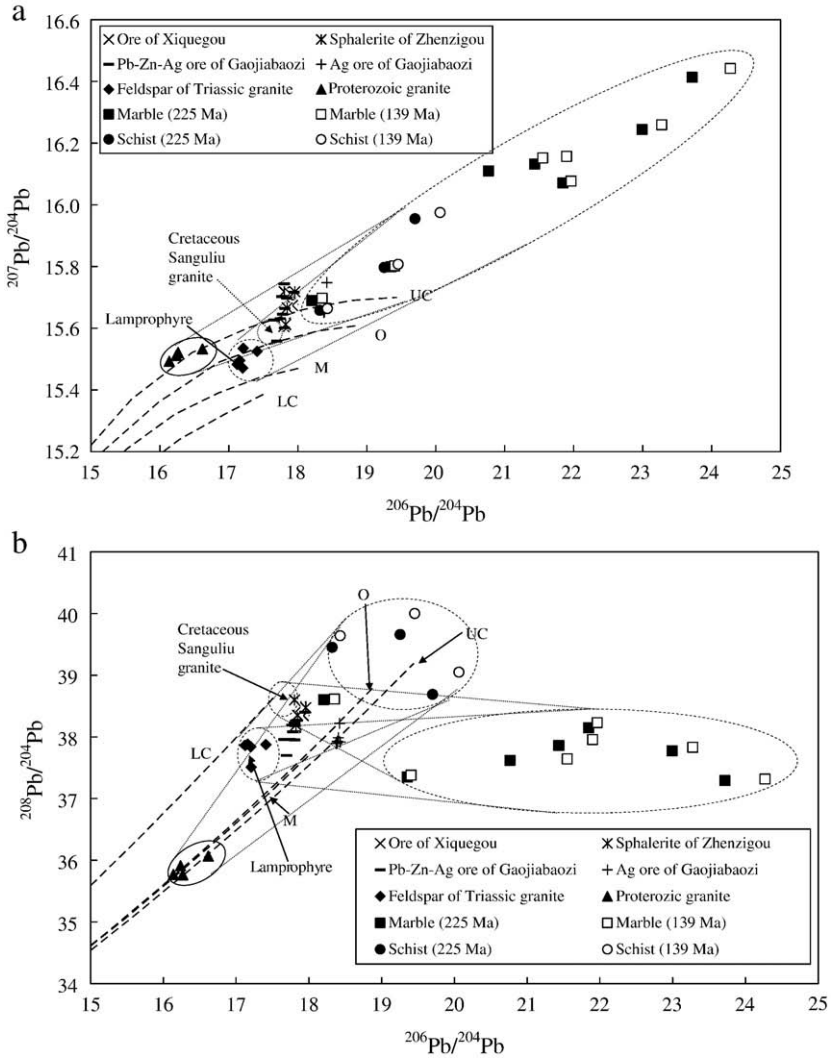

Fig. 9. Pb isotopic evolution diagram of the ores, feldspar of the Mesozoic granites, and the Proterozoic granites, marble, and schist of the Liaohe Group at Qingchengzi. a) $^{206}Pb/^{204}Pb$ *vs.* $^{207}Pb/^{204}Pb$ plot; b) $^{206}Pb/^{204}Pb$ *vs.* $^{208}Pb/^{204}Pb$ plot. The Pb isotopic evolution curves are based on Zartman and Doe (1981). UC: the upper crust; O: orogene; M: mantle; LC: lower crust. (225 Ma) and (139 Ma) stand for Pb isotopic ratios corrected for the 225 Ma and 139 Ma in situ radiogenic Pb. For Proterozoic granite samples, the difference between the two corrected values is smaller than the symbols. Data of the lamprophyre is from Ding et al. (1992) and the field of the Cretaceous Sanguliu granite is based on Wei et al. (2003).

ratios of the metamorphic rocks of the Liaohe Group are very radiogenic: $^{206}Pb/^{204}Pb$ (225 Ma)=18.20 to 23.72, $^{207}Pb/^{204}Pb$ (225 Ma)=15.69 to 16.41, $^{208}Pb/^{204}Pb$ (225 Ma)=37.29 to 38.60 for the marble of the Dashiqiao Formation and $^{206}Pb/^{204}Pb$ (225 Ma)=18.32 to 19.70, $^{207}Pb/^{204}Pb$ (225 Ma)=15.66 to 15.96, and $^{208}Pb/^{204}Pb$ (225 Ma)=38.69 to 39.66 for schist from the Gaixian Formation.

Table 8
Sr and Nd isotopic results of intrusive and metamorphic rocks from the Qingchengzi orefield

No.	Sample	Rb (ppm)	Sr (ppm)	$^{87}Rb/^{86}Sr$	$^{87}Sr/^{86}Sr$	+/−	$^{87}Sr/^{86}Sr(t_1)$	$^{87}Sr/^{86}Sr(t_2)$	Sm (ppm)	Nd (ppm)	$^{147}Sm/^{144}Nd$	$^{143}Nd/^{144}Nd$	+/−	$^{143}Nd/^{144}Nd(t_1)$	ε_{Nd} (t_1)	$^{143}Nd/^{144}Nd(t_2)$	ε_{Nd} (t_2)	$T_{DM\ II}$* (Ga)
291	Dashiqiao marble	3.531	110.5	0.0925	0.713335	16	0.71304	0.71315	0.380	2.682	0.0856	0.511203	10	0.511077	-24.8	0.511125	-26.0	2.48
296	Dashiqiao marble	18.43	132.6	0.4029	0.728415	17	0.72713	0.72762	0.570	3.379	0.102	0.511293	10	0.511143	-23.5	0.511200	-24.6	2.64
663	Gaixian schist	198.1	65.30	8.866	0.811462	19	0.78309	0.79395	7.848	45.46	0.1043	0.511246	10	0.511092	-24.5	0.511151	-25.5	2.76
689	Gaixian schist	199.9	72.62	8.150	0.947701	21	0.92162	0.93160	3.092	17.04	0.1097	0.511384	9	0.511222	-22.0	0.511284	-22.9	2.64
670	Dadingzi granite	111.1	691.9	0.465	0.716436	14	0.71495	0.71552	0.393	1.791	0.133	0.511753	9	0.511557	-15.4	0.511632	-16.1	2.48
672	Dadingzi granite	125.2	671.1	0.540	0.717875	14	0.71615	0.71681	0.710	3.270	0.131	0.511712	9	0.511519	-16.2	0.511593	-16.9	2.51
676	Shuangdinggou granite	186.1	534.0	1.009	0.711958	15	0.70873	0.70996	4.793	38.53	0.0752	0.511647	11	0.511536	-15.9	0.511579	-17.2	2.29
678	Shuangdinggou granite	197.4	737.4	0.775	0.711025	15	0.70854	0.70949	6.406	50.57	0.0766	0.511684	10	0.511571	-15.2	0.511614	-16.5	2.23
681	Xinling granite	204.1	919.1	0.643	0.711100	16	0.70904	0.70983	5.788	43.48	0.0805	0.511664	8	0.511545	-15.7	0.511591	-16.9	2.27

t_1=225 Ma; t_2=139 Ma.
* The two stage Nd isotope model ages were calculated after Liew and Hofmann (1988). For the detail, see the text.

Please cite this article as: Yu, G., et al., Geochronological framework and Pb, Sr isotope geochemistry of the Qingchengzi Pb–Zn–Ag–Au orefield, Northeastern China, Ore Geology Reviews (2008), doi:10.1016/j.oregeorev.2008.11.009

Obviously, Pb from the Gaixian schist shows higher $^{208}Pb/^{204}Pb$ ratios than that from the Dashiqiao marble (Table 7; Fig. 9). 139 Ma-corrected Pb isotopic compositions of the Proterozoic granite and the metamorphic rocks show little shift comparing with that corrected for 225 Ma (Table 7; Fig. 9).

4.4. Rb, Sr, Sm, Nd concentrations and Sr, Nd isotopic ratios of the ores and the country rocks

Ores from different deposits at the Qingchengzi orefield show very different initial Sr isotopic ratios. The Rb–Sr isochron of the sphalerite from Zhenzigou yields an initial Sr isotopic ratio of $^{87}Sr/^{86}Sr$ (221 Ma)= 0.7075±0.0063 (Table 3; Fig. 6). Pyrite samples suffered from relatively weaker disturbance than the galena samples at Xiquegou; the pyrite samples yield $^{87}Sr/^{86}Sr$ (225 Ma) of 0.7149 to 0.7218 (Table 4). Pyrite samples of the Pb–Zn–Ag ore from the Gaojiabaozi deposit yield $^{87}Sr/^{86}Sr$ (225 Ma) of 0.7215 to 0.7235, hydrothermal calcite 0.7258 to 0.7304, and pyrargyrite 0.7105, respectively (Table 5). Pyrargyrite samples from the Ag ore at Gaojiabaozi yield an isochron with an initial $^{87}Sr/^{86}Sr$ (139 Ma) of 0.71803±0.00028 (Table 5; Fig. 8).

Triassic granites show low initial Sr isotopic ratios of $^{87}Sr/^{86}Sr$ (225 Ma)=0.7085 to 0.7090 and $^{87}Sr/^{86}Sr$ (139 Ma)=0.7095 to 0.7100, and negative ε_{Nd} (225 Ma)=−15.2 to −15.9 and ε_{Nd} (139 Ma)=−16.5 to −17.2. Two stage Nd isotopic model ages are 2.2 to 2.3 Ga (Table 8).

At 225 Ma, Proterozoic granites, marble of the Dashiqiao Formation, and schist of the Gaixian Formation show high and variable $^{87}Sr/^{86}Sr$ (225 Ma) ratios of 0.7150 to 0.7162, 0.7130 to 0.7271, and 0.7831 to 0.9216, respectively (Table 8). These rocks show ε_{Nd} (225 Ma) of −15.4 to −16.2, −23.5 to −24.0, and −22.0 to −24.5, respectively. $^{87}Sr/^{86}Sr$ (139 Ma) ratios and ε_{Nd} (139 Ma) values of these rocks are not very different from the $^{87}Sr/^{86}Sr$ (225 Ma) ratios and ε_{Nd} (225 Ma) values, respectively. Two stage Nd isotopic model ages for the Proterozoic granites are about 2.5 Ga, and for the metamorphic rocks of the Liaohe Group are 2.5 to 2.7 Ga (Table 8).

5. Discussion

5.1. Geochronological framework for magmatic events in the Qingchengzi orefield

Some new age data were recently published for igneous rocks that outcrop at Qingchengzi. Liu and Ai (2002) reported K–Ar ages of 130±1, 149±1 and 211±3 Ma for samples from three lamprophyre dykes collected at the Xiaotongjiabaozi gold deposit. Wu et al. (2005a) reported a SHRIMP zircon U–Pb age of 168±3 for the microdiorite at the Baiyun gold mine, and Wu et al. (2005c) reported TIMS zircon U–Pb ages of 224±1 and 220±1 Ma for the granite at Shuangyashan and diorite at Laojiandingshan. We obtained new SHRIMP zircon U–Pb ages for the Xinling granite (225.3±1.8 Ma) and Yaojiagou granite (184.5± 1.6 Ma). Each age of the intrusive body and dyke obtained by this and previous investigations at Qingchengzi has been assigned as a magmatic event. The reason for doing so is that these ages have been found not only in the orefield, but also in the adjacent regions. This correlation suggests that ages obtained by this and previous studies at Qingchengzi are reliable, that they are not isolated events but rather regional ones, and that the general assumption that dykes cropping out at the present surface imply deeply situated main intrusive bodies with the same ages is valid.

Integrating our data with that in the literature permits a multi-stage magmatism interpretation for Qingchengzi and adjacent regions. Magmatic activity took place in three periods, the Triassic, Jurassic, and Early Cretaceous; each event contains several magmatic pulses.

The Xinling granite (225.3±1.8 Ma; this work) and Shuangyashan granite (224±1 Ma; Wu et al., 2005c), both from Qingchengzi, and Laojiandingshan diorite at the south of the Shuangdinggou granite (220±1 Ma; Wu et al., 2005c), are all coeval Triassic intrusions. Slightly later intrusions are lamprophyre at Xiaotongjiabaozi (211± 3 Ma; Liu and Ai, 2002) and a monzogranite and its dioritic inclusions at Xiuyan (212±1 to 216±2 Ma; Wu et al., 2005c) as well as a diorite at Tongjiabaozi (214±2 Ma; Wu et al., 2005c), located about 60 km southwest of Qingchengzi.

The Jurassic magmatic stage contains several pulses. Early Jurassic intrusions include the Yaojiagou granitie at Qingchengzi (184.5± 1.6 Ma; this work) and the Hanjialing monzogranite (179±3 Ma; Wu et al., 2005a), located about 50 km west of Qingchengzi. Middle Jurassic intrusions include the microdiorite at Qingchengzi (168±3 Ma; Wu et al., 2005a) and the monzogranite at Hanjialing (163±5 Ma; Wu et al., 2005a). Later Jurassic intrusions include lamprophyre at Qingchengzi (149±1 Ma; Liu and Ai, 2002) and the Gaoliduntai granite located about 35 km east of Qingchengzi (156±5 Ma; Li et al., 2004a,b), as well as the lamprophyre at Huaziyu magnesite deposit about 70 km west of Qingchengzi (155±4 Ma; Jiang et al., 2005).

The Cretaceous magmatic stage is represented by the lamprophyre at Qingchengzi (130±1 Ma; Liu and Ai, 2002), the monzogranite at Chaoyang, about 30 km south of Qingchengzi (127±1, 128±1 Ma; Wu et al., 2005b), the Jiguanshan granite, located about 40 km southeast of Qingchengzi (131±2 Ma; Wu et al., 2005b), the Fenghuangshan granite from about 60 km southeast of Qingchengzi (130±2 Ma; Wu et al., 2005b), and the Sanguliu granite, from about 90 km southeast of Qingchengzi (120±2 Ma to 131±3 Ma; Wu et al., 2005b). Additionally, a whole rock K–Ar age of 140±3 Ma for the microdiorite dyke at Qingchengzi was compiled by Ye et al. (1986). Contemporaneous magmatism also occurred at the northern margin of the North China Craton. For example, granite with a TIMS zircon U–Pb age of 138±2 Ma, associated with the Anjiayingzi gold mine, is located about 450 km NWW of Qingchengzi (Li et al., 2004a,b), and a rhyolitic ignimbrite with a SHRIMP zircon U–Pb age of 135.4±1.6 Ma is present about 500 km west of Qingchengzi (Liu et al., 2003).

Thus, Qingchengzi is a focus of the Triassic, Jurassic, and Early Cretaceous magmatic activities. The open system behavior of the Rb–Sr isotopes of the sulfide minerals from Qingchengzi deposits is probably caused by the multi-stage magmatism and associated hydrothermal activities.

5.2. Geodynamic significance of the magmatic activities at Qingchengzi

The Triassic magmatism at Qingchengzi is a part of the Triassic alkaline intrusion belt in the northern margin of the North China Craton (Yan et al., 1999). Alkaline intrusions in the belt were formed by melting of the metasomatized mantle caused by extension of the lithosphere and upwelling of the asthenospheric mantle (Lin et al., 1992; Yan et al., 1999; Mao et al., 2005). The Saima nepheline syenite and Bailinchuan syenite are exposed about 70 km NEE of Qingchengzi (Lin et al., 1992; Wu et al., 2005c). Granites also occur in this belt, such as the 400 km^2 Dushan granite and small bodies around it, located 300 km west of Qingchengzi. They were formed by crustal melting induced by alkaline mafic magma (Luo et al., 2003, 2004). The Triassic intrusions at Qingchengzi show calc-alkaline affinities, negative ε_{Nd} (T) values and second stage Nd isotope model ages ($T_{DM\ II}$) slightly younger than the Proterozoic metamorphic rocks. These suggest that they are products of the crustal melting induced by the mantle magma, but with a small input of mantle material.

Although many models exist, we have adopted the model postulated by Wu et al. (2005a,b) and others (e.g., Jiang et al., 2005) to explain the geodynamic settings of the Jurassic and Cretaceous magmatisms at Qingchengzi because the spatial and temporal distribution of the Jurassic and Cretaceous igneous rocks in eastern China and southeastern Asia favors this model. Subduction of the Paleopacific plate resulted in crustal thickening and subsequent local lithospheric delamination, which resulted in the upwelling of asthenospheric mantle and formation of juvenile crust by

Please cite this article as: Yu, G., et al., Geochronological framework and Pb, Sr isotope geochemistry of the Qingchengzi Pb–Zn–Ag–Au orefield, Northeastern China, Ore Geology Reviews (2008), doi:10.1016/j.oregeorev.2008.11.009

underplating of mantle derived magma. A subsequent thermal event from the asthenosphere partially melted the underplated mafic rocks and pre-existing ancient crust, forming the mafic and felsic magmas. The giant Cretaceous igneous event was related to lithospheric delamination in eastern China and possibly aided by superplume activity associated with global-scale mantle upwelling. Mixing of mafic magma derived from the mantle and newly underplated crust and felsic magma formed by melting of the ancient crust is common.

5.3. Ore-forming events in the orefield

The Triassic is the most important metallogenic stage at Qingchengzi. Rb–Sr isochron age (221±12 Ma) yielded by sphalerite from Zhenzigou is consistent with the zircon U–Pb age (225.3±1.8 Ma) obtained for the Triassic Xinling granitic intrusion. Thus, the formation of the Zhenzigou deposit is probably genetically related to the Triassic magmatic-hydrothermal activity. Pb isotopic compositions of the sphalerite from Zhenzigou agree with those of the pyrite and galena from Xiquegou and the hydrothermal calcite and pyrite of the Pb–Zn–Ag ore from Gaojiabaozi (Chen et al., 2005), suggesting the same origin and perhaps the same formation age for the ores. Rb–Sr isotopic data of the pyrite from Xiquegou plot near the 225 Ma reference isochron (Fig. 7). Therefore, it is very likely that all Pb–Zn deposits at the Qingchengzi orefield and the Pb–Zn–Ag ore at the Gaojiabaozi deposit were formed at the same time. Additionally, the Triassic age of the Pb–Zn–Ag ore at Gaojiabaozi is supported by the Rb–Sr isochron age of 234±12 Ma and the Ar-Ar age of 238.80±0.60 Ma, both from fluid inclusions in the vein quartz (Xue et al., 2003). Rb–Sr isochron age (233±31 Ma; Xue et al., 2003) yielded by gold-bearing silicic rocks has been interpreted as the formation age of the Xiaotongjiabaozi gold deposit, while the Ar–Ar age of 167±2 Ma yielded by sericite from the same deposit (Liu and Ai, 2002) represents the later thermal disturbance because of low closure temperature for Ar diffusion in fine grained sericite. Liu and Ai (2000) suggested that the Baiyun gold deposit also formed in the Triassic.

Several ore deposits associated with Triassic alkaline intrusions occur at the northern margin of the North China Craton, including the apatite-magnetite deposit associated with the Fangshan layered pyroxinite-syenite complex (218±8 Ma, Rb–Sr isochron age; Yan et al., 1999) and the uranium deposit associated with the Saima nepheline syenite (233±1 Ma, zircon U–Pb age; Wu et al., 2005c). Combined with the deposits at Qingchengzi, we suggest that the Triassic was an important metallogenic stage in the northern margin of the North China Craton.

The period of 190 to 160 Ma corresponds to a major Mesozoic metallogenic pulse in the northern margin of the North China Craton (Mao et al., 2005). Many Au, Ag, and Mo deposits in the region, and the Shanmen Ag deposit situated in the southern margin of the Xing'an Mongolian Orogenic Belt, just north of the North China Craton, were formed in this time interval (Liang et al., 2001; Mao et al., 2005). However, most Au ore deposits in eastern China were formed around 130 to 120 Ma (Yang et al., 2003; Mao et al., 2005), and a few around 140 Ma (Mao et al., 2005).

On the contrary, Jurassic mineralization is very weak at Qingchengzi, and only thermal overprinting caused by this thermal event can be seen in places in the orefield. For example, resetting of the K–Ar isotopic system of the sericite at Xiaotongjiabaozi (Liu and Ai, 2002) was probably caused by the 168±3 Ma magmatic activity (Wu et al., 2005c).

The period between about 130 Ma to 150 Ma is another important Mesozoic metallogenic pulse in North China. Many Mo, Cu, and Au deposits formed in the periphery of the North China Craton in this pulse (Mao et al., 2005). The formation of Ag ore at Gaojiabaozi may relate to the 130 to 150 Ma magmatic event. Small dykes may not have provided sufficient heat and metallogenic materials for ore genesis. However, we agree with Wu et al. (2005a,b) that mafic and felsic magmas were often generated in the same thermal event during Jurassic and Early Cretaceous igneous activities. The 140 Ma microdiorite dyke is very likely associated with a larger contemporaneous felsic intrusion(s) at depth. Hydrothermal fluid driven by these deeply situated large intrusive bodies, but not by dykes themselves, was responsible for the formation of the silver ore in Gaojiabaozi. Multistage hydrothermal activities have been found at other ore deposits, for example, the Shkol'noe Au–Ag deposit, Tadjikistan (Moralev and Shatagin, 1999) and the Shanggong gold deposit in China (Chen et al., 2008).

5.4. Sources of ore-forming materials

Since they are heavy elements, Sr and Pb isotopes do not fractionate during ore-forming processes. Therefore, changes of Sr and Pb isotopic ratios in hydrothermal fluids must be caused by the mixing of Sr and Pb from igneous rocks and metamorphic rocks. Two types of ore Pb with different isotopic compositions have been recognized at Qingchengzi. The first type is the Pb of the Pb–Zn ores from the Zhenzigou, Xiquegou, and other Pb and Zn deposits, as well as the Pb–Zn–Ag ore from Gaojiabaozi. They show very similar Pb isotopic ratios, with $^{206}Pb/^{204}Pb$=17.66 to 17.96, $^{207}Pb/^{204}Pb$=15.56 to 15.74 and $^{208}Pb/^{204}Pb$=37.70 to 38.60 (Chen et al., 2005), suggesting that they are derived from the same source. The second type is represented by the Pb in the Ag ore of the Gaojiabaozi deposit, with $^{206}Pb/^{204}Pb$=18.38 to 18.53, $^{207}Pb/^{204}Pb$=15.65 to 15.79 and $^{208}Pb/^{204}Pb$=37.89 to 38.34 (Table 6). They show a higher $^{206}Pb/^{204}Pb$ ratio, and therefore a younger model age. The different initial Pb isotopic compositions suggest that the two kinds of ore Pb were derived from different sources.

Pb isotopic ratios of the potassium feldspar sample from a lamprophyre at Qingchengzi ($^{206}Pb/^{204}Pb$=17.178, $^{207}Pb/^{204}Pb$=15.464, $^{208}Pb/^{204}Pb$=37.664; Ding et al., 1992) agree with the ranges of the Triassic granites, which suggests that Pb isotopic compositions of the Mesozoic granitic and mafic rocks may not vary significantly at Qingchengzi. This phenomenon is also observed at other locations in eastern China. For example, Mesozoic basaltic rocks and granitic rocks occurring along the Mid-Lower Yangtze region, south of the North China Craton show similar Pb isotopic ratios (Yan et al., 2005; Xie et al., 2007).

Pb of the Pb–Zn–(Ag) ores plot close to the field of the Triassic granite in the Pb isotopic diagram (Fig. 9). However, the ore Pb shows higher $^{206}Pb/^{204}Pb$, $^{207}Pb/^{204}Pb$, and $^{208}Pb/^{204}Pb$ ratios than the Pb of the Triassic granites; thus, a component with high $^{206}Pb/^{204}Pb$, $^{207}Pb/^{204}Pb$, and $^{208}Pb/^{204}Pb$ must have been involved in the formation of the ores. That component is very likely the Pb from the metamorphic rocks in the region, which show a radiogenic nature (Table 7; Fig. 9). Mass balance considerations suggest that the ore Pb is dominated by the Pb from the Triassic granites because the field of the ore Pb is close to that of the Pb from the granites but far from the average Pb isotopic compositions of the metamorphic rocks. Pb from the Proterozoic granite contributes little to the ore source because of the low Pb isotopic ratios, although its contribution cannot be entirely ruled out. Furthermore, Pb from the marble of the Dashiqiao Formation shows a lower $^{208}Pb/^{204}Pb$ ratio than that of Pb from the schist of the Gaixian Formation (Table 7, Fig. 9b), suggesting a lower Th/Pb ratio of the source. The ore lead, especially that from Zhenzigou and Xiquegou, plots between the fields of the Triassic granite and the schist of the Gaixian Formation but deviates from the tie line of the Triassic granite and the marble of the Dashiqiao Formation (Fig. 9b), suggesting that the schist of the Gaixian Formation is a more plausible source for the ores from Qingchengzi.

The different Pb isotopic compositions of the Pb–Zn–(Ag) and Ag ores may have resulted from the different lead contributions from the Triassic granites and from different metamorphic rocks. As discussed above (Section 5.3), the main granitic intrusion situated in the deep

Please cite this article as: Yu, G., et al., Geochronological framework and Pb, Sr isotope geochemistry of the Qingchengzi Pb–Zn–Ag–Au orefield, Northeastern China, Ore Geology Reviews (2008), doi:10.1016/j.oregeorev.2008.11.009

crust, and not the dykes, was responsible for the formation of the silver ore at Gaojiabaozi. However, the hidden intrusion is inaccessible and cannot be sampled. If we suppose that the deeply situated main intrusion possesses the same Pb isotopic compositions as the Triassic granites, the source of the silver ore is also material derived from the granitic intrusions and metamorphic rocks of the Liaohe Group, similar to that of the Pb–Zn ores but in different proportions. However, this may also be caused by different Pb isotopic compositions of the intrusion(s) responsible for the formation of the silver ore. In this regard, we may assume that the Pb isotopic ratios of the Sanguliu granite ($^{206}Pb/^{204}Pb$ = 17.496 to 17.717, $^{207}Pb/^{204}Pb$ = 15.552 to 15.621, $^{208}Pb/^{204}Pb$ = 38.521 to 39.749; Wei et al., 2003), which is 90 km SE of the Qingchengzi orefield and about 130 Ma in age, is approximately that of the hidden Cretaceous intrusion genetically related to the Ag ore at Gaojiabaozi. Pb isotopic ratios of the Sanguliu granite are higher than those of the Triassic granites at Qingchengzi (Fig. 9). Making this approximation, the difference in the Pb isotopic ratios of the Pb–Zn–(Ag) ore and the silver ore can be a result of the difference in the Pb isotopic compositions of the Triassic and Cretaceous intrusions, or the addition of Pb from the Cretaceous intrusion. If this is the case, Pb from the marble of the Dashiqiao Formation may also contribute to the Ag ore if $^{208}Pb/^{204}Pb$ is taken into account (Fig. 9b).

The implications of the Pb isotopic compositions of the metamorphic rocks of the Liaohe Group for the Precambrian geochronology of the region will be discussed elsewhere.

Strontium, a lithophile element, behaves differently from Pb, which is a chalcophile element. The Sr concentration is higher in the Dashiqiao marble than that in the Gaixian schist (Table 8). Moreover, Sr in the marble is more soluble than that in the schist. Sr in the schist can be released by decomposition of the Ca (therefore, Sr) bearing minerals, that is, by hydrothermal alteration of the rocks. However, wall rock alteration is weak at Qingchengzi. Thus, the Sr is mostly from the marble.

In the $^{87}Sr/^{86}Sr(t)$ *vs.* $^{206}Pb/^{204}Pb$ plot (Fig. 10), Pb–Zn ores of the Xiquegou and Zhenzigou deposits plot between the field of the Triassic granite and that of the marbles of the Dashiqiao Formation. Therefore, the Sr–Pb isotopes also suggest a derivation of Sr of the ores from Sr of the Triassic granite and of the metamorphic rocks. However, high $^{87}Sr/^{86}Sr(t)$ values of Pb–Zn–Ag ore and hydrothermal calcite from Gaojiabaozi require an involvement of Sr from the schist of the Gaixian Formation with very high $^{87}Sr/^{86}Sr(t)$ (Fig. 10). Strong wall rock alteration may be the mechanism for Sr to be released from the schist of the Gaixian Formation to enter the ores. We cannot determine if the Proterozoic granite provided the ore-forming materials based on the Pb and Sr isotopic relations.

As discussed above, the initial $^{87}Sr/^{86}Sr$ ratio of the 140 Ma magmatic event cannot be constrained because these granites are inaccessible. The $^{87}Sr/^{86}Sr(t)$ value of the 130 Ma Sanguliu granite (0.71482; Wei et al., 2003) is too high to be an approximate end-member of the mixed source for the Ag ore of Gaojiabaozi, because of the relatively low $^{87}Sr/^{86}Sr$ (139 Ma) of 0.70803 for the Ag ore. The Ag ore plots between the field of the Triassic granite and that of the marble of the Dashiqiao Formation. Therefore Sr of the Ag ore may be a mixture of Sr from the Triassic granites and from the marble of the Dashiqiao Formation, but with different proportions than the Triassic Pb–Zn–(Ag) ores, which is suggested by the different Pb isotopic ratios.

The mixed source for the ore-forming materials is supported by the trace element concentrations in the granites and in the metamorphic rocks. The Triassic Xinling and Shuangdinggou granite are enriched in Pb (45.8 and 53 ppm, number of averaged samples n = 11 and 34, respectively), Zn (124 and 112 ppm, n = 11 and 34), Ag (300 and 340 ppb, n = 11 and 34), and Au (4.5 and 7.2 ppb, n = 11 and 34; Fang et al., 1994) compared with the average composition of the upper crust (Pb = 28 ± 4 ppm, Zn = 67 ± 6 ppm, Ag = 53 ± 3 ppb and Au = 1.5 ± 0.4 ppb, respectively; Rudnick and Gao, 2004). On the other hand, the Jurassic Yaojiagou granite is not enriched in Pb (25 ppm, n = 9), but is slightly enriched in Zn (86 ppm, n = 9), and the Proterozoic Dadingzi granite is depleted in Pb (16 ppm, n = 25) and Zn (8 ppm, n = 25), but enriched in Au (4 ppb, n = 25; Fang et al., 1994). The metamorphic rocks of the Dashiqiao Formation are also enriched in Pb and Zn, especially the ore-bearing beds, which contain Pb of 73 to 266 ppm and Zn of 30 to 123 ppm, respectively (Fang et al., 1994). High concentrations of Pb, Zn, Ag, and Au in both Triassic granites and the ore-bearing beds in the Dashiqiao Formation provided abundant ore-forming metals to the ore deposits at Qingchengzi.

The sphalerite at Zhenzigou has the lowest initial Sr isotopic ratio of 0.707, showing the dominance of the magmatic Sr, whereas sulfide minerals from Xiquegou and Gaojiabaozi show higher and variable initial Sr isotopic ratios, suggesting large contributions of Sr from the metamorphic rocks of the Liaohe Group. This can be explained by as follows. Because the Zhenzigou deposit is hosted by the lowest horizon of the Dashiqiao Formation, it therefore may be the closest to the Triassic granitic intrusion. Hydrothermal fluid circulated around

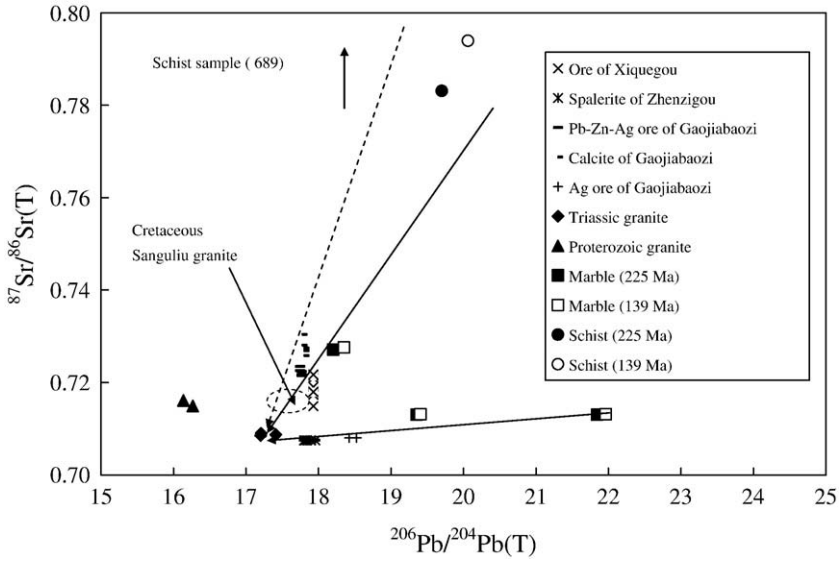

Fig. 10. $^{206}Pb/^{204}Pb$ *vs.* $^{87}Sr/^{86}Sr$ plot of the ores, feldspar of the Mesozoic granites, and the Proterozoic granites, marble, and schist of the Liaohe Group at Qingchengzi. (225 Ma) and (139 Ma) stand for Pb and Sr isotopic ratios corrected for the 225 Ma and 139 Ma in situ radiogenic Pb and Sr isotopes. For Proterozoic granite samples, the difference between the two corrected values is smaller than the symbols. The field of the Cretaceous Sanguliu granite is from Wei et al. (2003).

Please cite this article as: Yu, G., et al., Geochronological framework and Pb, Sr isotope geochemistry of the Qingchengzi Pb–Zn–Ag–Au orefield, Northeastern China, Ore Geology Reviews (2008), doi:10.1016/j.oregeorev.2008.11.009

the granite moves a short distance to Zhenzigou, and the Sr in the hydrothermal fluid in Zhenzigou is dominated by Sr from the granites. The Xiquegou deposit is hosted by the middle horizon of the Dashiqiao Formation, and hydrothermal fluid from the granite moves a moderate distance to Xiquegou deposit, leaches the metamorphic rocks to a larger degree, and contains more Sr from the metamorphic rocks. The Pb–Zn–Ag ore of Gaojiabaozi is hosted by the upper horizons of the Dashiqiao Formation, and the granite-driven hydrothermal fluid has to move a long distance to the deposit and thus leaches more Sr from the metamorphic rocks.

On the other hand, ores from Qingchengzi show relatively homogeneous Pb isotopic compositions and highly variable Sr isotopic ratios. This is most notably shown by the ore minerals of the Pb–Zn–Ag ore from Gaojiabaozi; these minerals show consistent $^{206}Pb/^{204}Pb$ ratios ranging from 17.65 to 17.84 (Chen et al., 2005), but variable $^{87}Sr/^{86}Sr$ ratios ranging from 0.7105 to 0.7304. Several reasons are postulated to explain the phenomena. First, ore Pb is dominated by Pb from the magmatic source at Qingchengzi. Second, Pb is a principle component of the dominant sulfide minerals in the ores. The sulfides are closely connected each other in the ores, and Pb can diffuse and be exchanged between these minerals quickly during cooling of the ores so that Pb isotopic equilibrium can be easily achieved. However, Sr exists mostly in the fluid inclusions, which are separated from each other. Sr cannot diffuse and be exchanged between disseminated inclusions during cooling of the ores to achieve Sr isotopic equilibrium (Yang et al., 2008). Moreover, the Pb isotopic system is highly resistant to later disturbance because Pb is a major component. In contrast, Sr isotopes can be easily disturbed because Sr is a trace component. Therefore, large variations in Sr isotopic ratios could result from the later disturbance. This explains why there are only a few cases in which homogeneous initial Sr isotope ratios remain in the sulfide minerals and Rb–Sr isotopic dating is possible. This also suggests that Sr isotopic equilibrium is easier to maintain at a small scale (for example, within a hand specimen) than at a large scale (for example, in the orebody), and the sub-sample technique is required (Yang et al., 2001).

5.5. Implications for the origin of deposits in the orefield

The Triassic and Early Cretaceous formation ages exclude the possibility that the deposits at Qingchengzi were formed by metamorphic processes (Zhang et al., 1984) or Proterozoic sea floor exhalation (Wang et al., 1994). Contemporaneous magmatism and mineralization at the Qingchengzi orefield suggest that the Mesozoic granite played a key role in the formation of the ore deposits. Granites in the orefield provided the heat which drove the circulation of the hydrothermal fluid around the intrusions. The Pb–Sr isotopic relations and the concentrations of the ore-forming elements of the ores, the granites, and the metamorphic rocks suggest that the hydrothermal fluid leached ore-forming materials from both Mesozoic granites and the metamorphic rocks of the Liaohe Group.

Several stages of concentration of ore-forming elements were involved in the formation of the ore deposits at Qingchengzi. High concentrations of Pb, Zn, Ag, and Au in the ore-bearing beds suggest that they were first enriched during the rift sedimentation because of the volcanic activities that occurred during the development of the rift in the Paleoproterozoic. Nd isotopic evidence suggests that the Triassic granite was formed by melting of the Paleoproterozoic metamorphic rocks with small input of the mantle-derived materials. Ore-forming elements were further enriched in the granite by melting of the metamorphic rocks with small amounts of the newly mantle-derived material. Hydrothermal fluid heated by the granitic intrusions leached the ore-forming elements from the Triassic (and Early Cretaceous) granites and the Paleoproterozoic metamorphic rocks. These ore-forming element-bearing fluids deposited those elements in the interbed fractures in the metamorphic rocks of the Liaohe Group. In this regard, we support the sedimentation-(metamorphism)-hydrothermal reworking model (Jiang, 1987, 1988; Jiang and Wei, 1989; Ding et al., 1992) that suggests that the deposits were formed in the Mesozoic (Liu and Ai, 2002; Xue et al., 2003).

Triassic granitic stocks and batholiths crop out at the western part of the Qingchengzi orefield, while magmatic activities with younger ages (ranging from ca. 210 to 130 Ma) are all represented by dykes throughout the orefield. Therefore, we suggest that the hydrothermal fluid driven by the heat provided by the Triassic intrusion(s) could have easily reacted with the marbles and schists near the intrusions and deposited ore-forming elements to form the mesothermal Zn–Pb deposits in the west part of the field. Hydrothermal fluids driven by deeply situated younger intrusions could not reach to the present surface, and thus no ore deposits are associated with these magmatic activities. In the eastern part of the orefield, hydrothermal fluids associated with the deeply situated Triassic intrusions could move upward along the Jianshanzi fault and deposited the ore-forming elements in the upper horizons of the Dashiqiao Formation to form the epithermal Au and Pb–Zn–Ag ores in the Triassic. Young, deeply situated intrusions with ages of ca. 140 Ma were probably larger or shallower, and thus sufficient amount of fluids were able to reach to the present surface and were responsible for the formation of the silver ore in the Gaojiabaozi deposit.

5.6. Implications for Rb–Sr dating of hydrothermal sulfide deposits

Re–Os dating has proven to be a powerful geochronological tool for dating sulfide minerals (Shirey and Walker, 1998). However, many sulfide minerals, such as those at Qingchengzi, contain less than 1 ppt Os, which is difficult to be measured precisely. In this case, Rb–Sr dating of the sulfide minerals, mostly sphalerite and pyrite, is often used to date the formation time of hydrothermal deposits (Brannon et al., 1992; Nakai et al., 1990, 1993; Christensen et al., 1995a,b; Hou et al., 2006; Han et al., 2007; Wei et al., 2003; Yang and Zhou, 2001). However, such an exercise is not always successful. Many factors affect Rb–Sr dating of sulfide minerals (Pettke and Diamond, 1996). Among these factors, previous work has suggested that a separation of the fluid inclusion from the "sulfide" phases (which may contain some primary fluid inclusions in it) is necessary. Usually, the "sulfide" phases yield relatively precise and meaningful isochrons, although the chemical state of Rb and Sr in sulfide minerals is unclear. Previous studies crushed samples in water and washed the 200 mesh mineral powder with dilute acids so as to separate secondary inclusions (Brannon et al., 1992; Nakai et al., 1990, 1993; Christensen et al., 1995a,b; Yang and Zhou, 2001). Our work suggested that leaching the mineral powder by 0.2 M HCl is successful in obtaining geologically meaningful isochrons.

Moreover, we first obtained an Rb–Sr isochron for pyrargyrite from the Gaojiabaozi Ag deposit. We suggest that pyrargyrite is a promising mineral to be used to date the mineralization age of the Ag deposits in the future although more work is needed to verify the geological significance of the apparent age.

6. Conclusions

A multi-stage magmatism, extending from the Proterozoic to the Triassic, Jurassic, and Early Cretaceous, occurred at the Qingchengzi orefield, where Pb–Zn and Ag–Au deposits are clustered. Pb–Zn deposits, Pb–Zn–Ag ore of the Gaojiabaozi deposit, and gold deposits, as well as the Xinling and Shuangdinggou granite intrusions, were formed contemporaneously in the Triassic (ca. 225 Ma). The close temporal and spatial relations suggest a probable genetic link between the ore- and rock-forming processes. The silver ore of the Gaojiabaozi deposit was formed at 138.7 ± 4.1 Ma. The formation of the silver ore is very likely related to 140 Ma magmatic activity, which is represented by dykes, but it was the contemporaneous large deep intrusive bodies, not the dykes, that were responsible for the formation of the silver ore.

Please cite this article as: Yu, G., et al., Geochronological framework and Pb, Sr isotope geochemistry of the Qingchengzi Pb–Zn–Ag–Au orefield, Northeastern China, Ore Geology Reviews (2008), doi:10.1016/j.oregeorev.2008.11.009

Pb and Sr isotopic ratios suggest that the ore-forming materials of the deposits at the Qingchengzi orefield were derived from a mixed source in which the Mesozoic intrusions were dominant and the Proterozoic metamorphic rocks (more likely the schist of the Gaixian Formation) were minor.

Mesozoic granitic intrusions played a key role in the generation of the deposits at Qingchengzi. They provided the heat which resulted in the formation of the hydrothermal circulation system, which in turn leached ore-forming materials from the granites themselves and Proterozoic metamorphic rocks. In the western part of the orefield, fluids driven by the Triassic granites moved a short distance to deposit Pb and Zn in the lower and middle horizons of the Dashiqiao Formation to form mesothermal deposits. In the eastern part of the field, Triassic granites are situated at a deeper level, and the fluids driven by these granites moved along the Jianshanzi fault over a long distance to deposit Ag and Au in the upper horizons of the Dashiqiao Formation to form epithermal deposits. Among the young igneous bodies, only the 140 Ma intrusive body is large enough to drive fluids to leach ore-forming elements from the granite and the surrounding rocks to form the Ag ore. Our new data support the sedimentation-hydrothermal reworking model for deposits at Qingchengzi (Jiang, 1987, 1988; Jiang and Wei, 1989; Ding et al., 1992; Liu and Ai, 2002; Xue et al., 2003). Multi-stage magmatism and mineralization disturbed the isotopic systems of the deposits, which interferes with the isotopic dating of these deposits.

Our work suggest that the step-dissolution Rb–Sr dating technique is capable of dating many sulfide minerals, such as sphalerite, pyrite, and pyrargyrite, from hydrothermal ore deposits, and that pyrargyrite is a promising mineral to be used to date the formation of silver deposit, although more work is needed.

Acknowledgements

We thank Mr. Zhanxing Yang of the Geological Survey of Liaoning Province, Mr. Fude Gao of the Qingchengzi Pb–Zn Mining Company, Mr. Tiejun Hu, and Lianzhong Yang of the 103 Geologic Team of the Non-ferrous Metal Company, and Mr. Xiyang Wang, Guowei Yang, and Wenju Ma of the Fengcheng Silver Mining Company for assistance in the field work. We thank Prof. Liu D.Y., and Dr. Shi Y.R. of the Chinese Academy of Geological Sciences for assistance in the zircon SHRIMP dating, Prof. Chen S.Y., Yu H.M., and Sun M. of USTC for assistance in the trace element measurements by ICP-MS, and Prof. Peng Z.C., and Mr. He J.F. of USTC for assistance with the mass-spectrometry. This work was supported by the State Key Basic Research Program (Grant No. 19990432301) and the Hefei Analysis Foundation of Chinese Academy of Sciences. We also thank Dr. Franco Pirajno and an anonymous reviewer, as well as Associate Editor, Dr. Jingwen Mao for offering comments which have substantially improved the manuscript.

References

103GT (103 Geological Team and Research Group on Geology of Qingchengzi Pb Deposits), 1976. General Report of Geology of the Qingchengzi Area (1970–1975). Internal report, 175 pp. (in Chinese).

Bouse, R.M., Ruiz, J., Tilley, S.R., Tosdal, R.M., Wooden, J.L., 1999. Lead isotope compositions of Late Cretaceous and Early Tertiary igneous rocks and sulfide minerals in Arizona: Implications for the sources of plutons and metals in porphyry copper deposits. Economic Geology 94, 211–244.

Brannon, J.C., Podosek, F.A., McLimans, R.K., 1992. Alleghenian age of the upper Mississippi Valley zinc-lead deposit determined by Rb–Sr dating of sphalerite. Nature 356, 509–511.

Chen, J.F., Jahn, B.M., 1998. Crustal evolution of southeastern China: Evidence from Nd and Sr isotopic compositions of rocks. Tectonophysics 284, 101–133.

Chen, J.F., Jahn, B.M., 1999. Nd, Sr and Pb isotopic systematics and evolution of the continental crust of southeastern China. In: Zheng, Y.F. (Ed.), Collections on chemical geodynamics. Science Press, Beijing, pp. 262–287 (in Chinese).

Chen, Y.W., Mao, C.X., Zhu, B.Q., 1980. Lead isotopic composition and genesis of Phanerozoic metal deposits in China. Geochimica 9, 215–229 (in Chinese).

Chen, J.F., Yu, G., Xue, C.J., Qian, H., He, J.F., Xing, Z., Zhang, X., 2005. Pb isotope geochemistry of lead, zinc, gold and silver deposit clustered region, Liaodong rift zone, northeastern China. Science in China Series D 48, 467–476.

Chen, Y.J., Pirajno, F., Qi, J.P., 2008. The Shanggong gold deposit, Eastern Qinling Orogen, China: Isotope geochemistry and implications for ore genesis. Journal of Asian Earth Science, 33, 252–266.

Christensen, J.N., Halliday, A.N., Leigh, K.E., Randeli, R.N., Kesler, S.E., 1995a. Direct dating of sulfides by Rb–Sr: A critical test using the Polaris Mississippi Valley-type Zn–Pb deposit. Geochimica et Cosmochimica Acta 59, 5191–5197.

Christensen, J.N., Halliday, A.N., Vearncombe, J.R., Kesler, S.E., 1995b. Testing models of large-scale crustal fluid flow using direct dating of sulfides: Rb–Sr evidence for early dewatering and formation of Mississippi Valley type deposits, Canning Basin, Australia. Economic Geology 90, 877–884.

Chu, X.L., Huo, W.G., Zhang, X., 2001. Sulfur, carbon and lead isotope studies of the Dajing polymetallic deposit in Linxi County, Inner Mongolia, China — Implications for metallogenic elements from hypomagmatic source. Resource Geology 51, 333–344.

Compston, W., Williams, I.S., Kirschvink, J.L., Zichao, Z., Guogan, M.A., 1992. Zircon U–Pb ages for the Early Cambrian time-scale. Journal Geological Society of London 149, 171–184.

Ding, T.P., Jiang, S.Y., Wan, D.F., Li, J.C., Song, B., Zhao, D.M., 1992. Stable isotope studies on the Proterozoic Pb–Zn mineral belt of northern China. Beijing Publishing House of Science and Technology, Beijing, pp. 36–60 (in Chinese).

Fang, R.H., He, S.S., Fu, D.B., 1994. Nonferrous metallic ore deposit in the east Liaoning–south Jilin early Proterozoic rift. In: Rui, Z.Y., Shi, L.D., Fang, R.H. (Eds.), Geology of nonferrous metallic deposits in the northern margin of the North China Landmass and its adjacent area. Geological Publishing House, Beijing, pp. 54–109 (in Chinese).

Faure, M., Lin, W., Monie, P., Bruguier, O., 2004. Paleoproterozoic arc magmatism and collision in Liaodong Peninsula (north-east China). Terra Nova 16, 75–80.

Foland, K.A., Allen, J.C., 1991. Magma sources for Mesozoic anorogenic granites of the White Mountain magma series, New England USA. Contributions to Mineralogy and Petrology 109, 195–211.

Geological Institute of Non-ferrous Metal Deposits of Liaoning Province, 1990. Geological Map of the Qingchengzi Region. Internal report.

Han, Y.G., Li, X.H., Zhang, S.H., Zhang, Y.H., Chen, F.K., 2007. Single grain Rb–Sr dating of euhedral and cataclastic pyrite in the Qiyugou gold deposit in western Henan, central China. Chinese Science Bulletin 52 (13), 1820–1826.

Hou, M., Jiang, S.Y., Jiang, Y.H., Ling, H.F., 2006. S–Pb isotope geochemistry and Rb–Sr geochronology of the Penglai gold field in the eastern Shandong province. Acta Petrologica Sinica 22 (10), 2525–2533 (in Chinese with English abstract).

Jiang, S.Y., 1987. Pb isotope composition at Qingchengzi lead-zinc deposit and its geological application. Journal of Peking University (Natural Science) 23 (4), 112–119 (in Chinese).

Jiang, S.Y., 1988. O, C, Pb, S isotopic characteristics and the origin of the Qingchengzi Pb–Zn deposits, Liaoning Province. Geological Review 34, 515–523 (in Chinese).

Jiang, S.Y., Wei, J.Y., 1989. Geochemistry of the Qingchengzi Pb–Zn deposits. Mineral Deposits 8, 20–28 (in Chinese).

Jiang, Y.H., Jiang, S.Y., Zhao, K.D., Ni, P., Lin, H.F., Liu, D.Y., 2005. SHRIMP U–Pb zircon dating for lamprophyre from Liaodong Peninsula: Constraints on the initial time of Mesozoic lithosphere thinning beneath eastern China. Chinese Science Bulletin 50 (22), 2612–2620.

Li, S.Z., Zhao, G.C., Wu, F.Y., 2004a. Mesozoic, not Paleoproterozoic SHRIMP U–Pb zircon ages for two Liaoji granites, eastern block, North China craton. International Geology Review 46, 162–176.

Li, Y.G., Zhai, M.G., Yang, J.H., Miao, L.C., Guan, H., 2004b. Gold mineralization age of the Anjiayingzi gold deposit in Chifeng County, Inner Mongolia and implications for Mesozoic metallogenic explosion in North China. Science in China Series D 47, 115–121.

Liang, Y., Wang, X.Z., Cheng, J.P., 2001. Rb–Sr isotope age and the time scale of hydrothermal activities for the Siping Ag(Au) deposit, Jilin Province. Geotectonica Metallogenia 25 (2), 194–198 (in Chinese with English abstract).

Liew, T.C., Hofmann, A.W., 1988. Precambrian crustal components, plutonic assimilations, plate environment of the Hercynian Fold belt of central Europe: Indications from a Nd and Sr isotopic study. Contributions to Mineralogy and Petrology 98, 129–138.

Lin, J.Q., Tan, D.J., Chi, X.G., Bi, L.J., Xie, C.F., Xu, W.L., 1992. Mesozoic granites in Jiao-Liao Peninsula. Science Press, Beijing. 208 pp., (in Chinese).

Liu, G.P., 1998. Studies on geological and geochemical characteristics of major gold deposits in Qingchengzi, eastern Liaoning province. Ph. D. Dissertation, Beijing, Peking University, 63 pp.

Liu, G.P., Ai, Y.F., 2000. Studies on the mineralization age of Baiyun gold deposit in Liaoning. Acta Petrologica Sinica 16 (4), 627–632 (in Chinese with English abstract).

Liu, G.P., Ai, Y.F., 2002. Study on ore-forming epoch of Xiaotongjiabaozi gold deposit, Liaoning Province. Mineral Deposits 21, 53–57 (in Chinese).

Liu, G.P., Ai, Y.F., Xian, W.S., 1997. Geochemical characteristics of lamprophyre from the Taoyuan-Xiaotongjiabaozi gold ore belt and their geological significance. Acta Petrologica Mineralogica 16 (4), 324–330 (in Chinese with English abstract).

Liu, G.P., Deng, Y.C., Zhou, G.X., 2001. Type of ore deposits and prospecting at the Qingchengzi ore field. Geological Survey of China. Symposium on Regional Geology and Metallogeny of Liaoning and Jilin Provinces, pp. 19–23 (in Chinese).

Liu, Y.C., Li, P.X., Tian, S.G., 2003. SHRIMP U–Pb zircon age of Late Mesozoic tuff (Lava) in Luanping basin, northern Hebei, and its implications. Acta Petrologica Mineralogica 22 (3), 237–244 (in Chinese with English abstract).

Lu, X.P., Wu, F.Y., Guo, J.H., Wilde, S.A., Yang, J.H., Liu, X.M., Zhang, X.O., 2006. Zircon U–Pb geochronological constraints on the Paleoproterozoic crustal evolution of the Eastern block in the North China Craton. Precambrian Research 146, 138–164.

Ludwig, K.R., 1997. Isoplot- A plotting and regression program for radiogenic-isotope data. Version 2.92, 47 pp.

Please cite this article as: Yu, G., et al., Geochronological framework and Pb, Sr isotope geochemistry of the Qingchengzi Pb–Zn–Ag–Au orefield, Northeastern China, Ore Geology Reviews (2008), doi:10.1016/j.oregeorev.2008.11.009

Luo, Z.K., Miao, L.C., Guan, K., Qiu, Y.S., Qiu, Y.M., McNaughton, N.J., Groves, D.I., 2003. SHRIMP U–Pb zircon dating of the Dushan granitic batholith and related granite–porphyry dyke, eastern Hebei Province, China, and their geological significance. Geochimica 32 (2), 173–180 (in Chinese with English abstract).

Luo, Z.K., Li, J.J., Guan, K., Qiu, Y.S., Qiu, Y.M., McNaughton, N.J., Groves, D.I., 2004. SHRIMP zircon U–Pb age of the granite at Baizhangzi gold field in Lingyuan, Liaoning Province. Geological Survey Research 27 (2), 82–85 (in Chinese with English abstract).

Mao, J.W., Xie, G.Q., Zhang, Z.H., Li, X.F., Wang, Y.T., Zhang, C.Q., Li, Y.F., 2005. Mesozoic large-scale metallogenic pulses in North China and corresponding geodynamic setting. Acta Petrologica Sinica 21 (1), 169–188 (in Chinese with English abstract).

Marcoux, E., Grancea, L., Lupulescu, M., Milesi, J.P., 2002. Lead isotope signatures of epithermal and porphyry-type ore deposits from the Romanian Carpathian Mountains. Mineralium Deposita 37, 173–184.

Moralev, G.V., Shatagin, K.N., 1999. Rb–Sr study of Au–Ag Shkol'noe deposit (Kurama Mountains, north Tadjikistan): age of mineralization and time scale of hydrothermal processes. Mineralium Deposita 34, 405–413.

Nakai, S., Halliday, A.N., Kesler, S.E., Jones, H.D., 1990. Rb–Sr dating of sphalerites from Tennessee and the genesis of Mississippi Valley type ore deposits. Nature 346, 354–357.

Nakai, S., Halliday, A.N., Kesler, S.E., Jones, H.D., Kyle, J.R., Lane, T.E., 1993. Rb–Sr dating of sphalerites from Mississippi Valley-type (MVT) ore deposits. Geochimica et Cosmochimica Acta 57, 417–427.

Pettke, K., Diamond, L.W., 1996. Rb–Sr dating of sphalerite based on fluid inclusion-host mineral isochrons: A clarification of why it works. Economic Geology 91, 951–956.

Rubatto, D., 2002. Zircon trace element geochemistry: Partitioning with garnet and the link between U–Pb ages and metamorphism. Chemical Geology 184, 123–138.

Rudnick, R.L., Gao, S., 2004. Composition of the continental crust. In: Rudnick, R.L., Holland, H.D., Turekian, K.K. (Eds.), Treatise on Geochemistry. The Crust, 3. Elsevier, Amsterdam, pp. 1–64.

Shirey, S.B., Walker, R.J., 1998. The Re–Os isotope system in cosmochemistry and high-temperature geochemistry. Annual Review of Earth and Planetary Science 26, 423–500.

Vavra, G., Gebauer, D., Schmid, R., Compston, W., 1996. Multiple zircon growth and recrystallization during polyphase Late Carboniferous to Triassic metamorphism in granulites of the Ivrea Zone (Southern Alps): An ion microprobe (SHRIMP) study. Contributions to Mineralogy and Petrology 122, 337–358.

Wang, W.Q., Qu, Y.J., 2000. Geological characteristics and metallogenic models of gold deposits of Paleoproterozoic in east Liaoning Province. Liaoning Geology 17 (3), 161–172 (in Chinese).

Wang, K.Y., Zhao, Y.M., Cao, X.L., 1994. The Proterozoic type lead-zinc deposits in northern border of North China platform. Geological Publishing House, Beijing. 190 pp., (in Chinese).

Wei, M., 2001. Geological characteristics and the origin of gold and silver deposits from the Qingchengzi ore field. Geological Survey of China. Symposium on Regional Geology and Metallogeny of Liaoning and Jilin Provinces, pp. 137–145.

Wei, J.H., Liu, C.Q., Tang, H.F., 2003. Rb–Sr and U–Pb isotopic systematics of pyrite and granite in Liaodong gold province, North China: Implication for the age and genesis of a gold deposit. Geochemical Journal 37, 567–577.

Wu, F.Y., Yang, J.H., Wilde, S.A., Zhang, X.O., 2005a. Geochronology, petrogenesis and tectonic implications of Jurassic granites in the Liaodong Peninsula, NE China. Chemical Geology 221, 127–156.

Wu, F.Y., Lin, J.Q., Wilde, S.A., Zhang, X.O., Yang, J.H., 2005b. Nature and significance of the early Cretaceous giant igneous event in eastern China. Earth and Planetary Science Letters 233, 103–119.

Wu, F.Y., Yang, J.H., Liu, X.M., 2005c. Geochronological framework of the Mesozoic granitic magmatism in the Liaodong Peninsula, Northeast China. Geological Journal of China Universities 11 (3), 305–317 (in Chinese with English abstract).

Xie, Z., Li, Q.Z., Chen, J.F., Gao, T.S., 2007. The geochemical characteristics of the Early-Cretaceous volcanics in Luzhong region and their source significance. Geological Journal of China Universities 13 (2), 235–249 (in Chinese with English abstract).

Xue, C.J., Chen, Y.C., Lu, Y.F., Li, H.Q., 2003. Metallogenic epochs of Au and Ag deposits in Qingchengzi ore-clustered area, eastern Liaoning Province. Mineral Deposits, 22, pp. 177–184 (in Chinese).

Yan, G.H., Mu, B.L., Xu, B.L., He, G.Q., Tan, L.K., Zhao, H., He, Z.F., Zhang, R.H., Qiao, G.S., 1999. Triassic alkaline intrusives in the Yanliao–Yanshan area: their chronology, Sr, Nd and Pb isotopic characteristics and their implications. Science in China Series D 42, 582–587.

Yan, J., Chen, J.F., Xie, Z., Yang, G., Yu, G., Qian, H., 2005. Geochemistry of Late Mesozoic basalts from Kedoushan in the Middle and Lower Yangtze regions: Constraints on characteristics and evolution of the lithospheric mantle. Geochimica 34 (5), 455–469 (in Chinese with English abstract).

Yang, J.H., Zhou, X.H., 2001. Rb–Sr, Sm–Nd and Pb isotope systematics of pyrite: implications for the age and genesis of lode gold deposits. Geology 29, 711–714.

Yang, J.H., Wu, F.Y., Wilde, S.A., 2003. A review of the geodynamic setting of large-scale Late Mesozoic gold mineralization in the North China Craton: an association with lithospheric thinning. Ore Geology Reviews 23, 125–152.

Yang, S.H., Qu, W.J., Tian, Y.L., Chen, J.F., Yang, G., Du, A.D., 2008. Origin of the inconsistent apparent Re–Os ages of the Jinchuan Ni–Cu sulfide ore deposit, China: Post-segregation diffusion of Os. Chemical Geology 247, 401–418.

Ye, B.D., Shen, Y.Z., Zhu, J.C., 1986. A compilation of the isotopic ages of China, vol. 4. Geological Publishing House, Beijing, pp. 284–285 (in Chinese).

Zartman, R.E., Doe, B.R., 1981. Plumbotectonics-the model. Tectonophysics 75, 135–162.

Zhang, Q.S., 1984. Geology and Metallogeny at Early Proterozoic in China. Jilin People's Press, Changchun. 536 pp., (in Chinese).

Zhang, L.G., 1995. Block geology of Eastern Asia lithosphere- Isotope geochemistry and dynamic of upper mantle, basement and granite. Science Press, Beijing. 252 pp., (in Chinese).

Please cite this article as: Yu, G., et al., Geochronological framework and Pb, Sr isotope geochemistry of the Qingchengzi Pb–Zn–Ag–Au orefield, Northeastern China, Ore Geology Reviews (2008), doi:10.1016/j.oregeorev.2008.11.009